Materials Advances

ROYAL SOCIETY OF CHEMISTRY

REVIEW

View Article Online
View Journal | View Issue

Cite this: *Mater. Adv.*, 2022, 3, 8063

Recent trends in covalent organic frameworks (COFs) for carbon dioxide reduction

Priyanka Sarkar, Ipsita Hazra Chowdhury, Surya Das and Sk. Manirul Islam *

As the ultimate carbon emission product of the combustion process, carbon dioxide (CO_2) is a serious environmental threat in increasing the global climate temperature through the greenhouse effect. Porous heterogeneous catalysts have attracted much attention for carbon capture and in the recent past; they have witnessed significant advancements in their design and implementation for the CO_2 capture and conversion. In this context, covalent organic frameworks (COFs), a kind of porous crystalline polymeric material, are mainly constructed by organic module units connected with strong covalent bonds. COFs, possessing unique properties such as low-density, large specific surface area, high thermal stability, and developed pore-structure and the long-range order, good crystallinity, and excellent tunability of the monomer units find versatile applications ranging from adsorption and separation, sensing, catalysis, optoelectronics, energy storage, and mass transport. In this review article, we discuss the emerging developments in different types of covalent organic frameworks (COFs) as heterogeneous catalysts for CO_2 reduction *via* photochemical, electrochemical, and photo coupled electrochemical pathways. The physicochemical properties of COFs and their influence on the efficiency, selectivity, and recyclability for CO_2 reduction are enlightened systematically. This review provides a concise report on various types of COFs, current trends, their application in CO_2 reduction for the synthesis of fuels and value-added fine chemicals, and future research directions for the deployment of COF catalysts in CO_2 capture and reduction.

Received 28th May 2022,
Accepted 20th September 2022

DOI: 10.1039/d2ma00600f

rsc.li/materials-advances

1. Introduction

Currently, one of the greatest worldwide calamities is global warming caused by the continuously increasing concentration of CO_2 in the atmosphere and ocean, which arises dramatically due to anthropogenic actions and the risk of ecosystem devastation.[1] Population growth and industrial progress contribute significantly to enhancing excessive CO_2 emissions unprecedentedly due to the escalating rate of carbon-based fuel consumption.[2] Therefore, it is vital to diminish the accumulation of one of the main greenhouse gases, CO_2, in the atmosphere

Department of Chemistry, University of Kalyani, Kalyani, Nadia 741235, WB, India. E-mail: manir65@rediffmail.com; Fax: +91-33-2582-8282; Tel: +91-33-2582-8750

Priyanka Sarkar

Ms Priyanka Sarkar is currently a PhD student at the University of Kalyani. She received her master's degree in science also from the University of Kalyani. Her current research focuses on the development of porous materials for CO_2 fixation reactions and other organic transformations.

Ipsita Hazra Chowdhury

Dr Ipsita Hazra Chowdhury is currently a research associate at the University of Kalyani. She received her PhD degree in Chemistry from CSIR-Central Glass and Ceramic Research Institute, Kolkata. She received her master's degree in science from IIEST, Shibpur. Her current research focuses on the development of porous polymers for the synthesis of valuable fine chemicals via CO_2 fixation and reduction reactions.

using effectual technologies or tactics.[3] To date, there are several ways to reduce emitted CO_2 concentration in the atmosphere, for instance, decreasing the amount of produced carbon-dioxide, growing green carbon sinks *e.g.*, plants, phytoplankton, and algae carrying chloroplasts, and capturing and storing up CO_2. To tackle the hazardous problems of global climate change along with sustainable energy shortage, it would be a more advantageous approach to efficiently capture and transform atmospheric CO_2 into useful carbon-based material or chemicals utilizing sustainable energy resources, forming a sustainable recycling system.[4] CO_2 is non-toxic, renewable, inexpensive, and most abundant raw C1 feedstocks and acts as a C1 building block for the synthesis of various valuable chemicals with added economic value.[4] The proper resolution to pacify our present demand and future energy supply is the conversion of CO_2 into valuable carbonaceous chemicals especially C1 and/or C2 products for example CO, CH_4, CH_3OH, C_2H_5OH, and other hydrocarbon compounds.[5] For this purpose, numerous catalytic systems and methods such as hydrothermal, electrochemical, and photochemical methods have been explored for the conversion of CO_2 to hydrocarbons having high catalytic efficiency, long-standing chemical stability, and non-toxicity, and low-cost materials. High temperature and pressure are required for the hydrothermal reduction process, which is energy intensive and expensive,[6] hence photochemical and electrochemical methods are the most prominent and green methods for CO_2 reduction, which shows a way for large-scale and long-lasting energy storage.[7] Direct electrochemical CO_2 reduction process is mainly achieved by changing parameters such as electrolytes and redox potential whereas the photocatalytic process is generally attributed to the slowest electron–hole recombination rate. In nature, the conversion of CO_2 occurs daily through the photosynthesis process in green plants to balance the global carbon/oxygen cycle. To retain this cycle mimicking of the natural photosynthesis process, in 1979 a number of semiconductor materials (WO_3, CdS, TiO_2, GaP, ZnO, and SiC) were investigated for the photo-catalytic CO_2 reduction in water to generate methanol, formic acid, formaldehyde and trace quantity of methane by Honda and his group.[8] Then, modifying semiconductors a number of photo/electrocatalytic systems have been studied so far and the catalytic system having high CO_2 adsorption capacity, good light absorbing ability, catalytic active sites, high selectivity, *etc.* are the main requirements for chemical reduction of CO_2. To date emerging trends of heterogeneous porous materials, covalent organic frameworks (COFs) performed as a versatile material, which shows prominent contribution in the field of catalysis for photo/electrocatalytic CO_2 reduction.[9] COFs, a series of covalently connected porous networks, which exhibit high crystallinity, porosity and a greater degree of modularity than several porous compounds, are generally constructed using the dynamic covalent chemistry theory.[10] A variety of methods have been involved in the preparation of COFs such as solvothermal,[11] microwave-assisted,[12] mechanochemical,[13] and vapor-assisted conversion.[14] However, in COF synthetic chemistry, the solvothermal method is the most well-known and usually utilized method. Owing to their ordered structure, highly accessible surface area, large pores, excellent thermal stability, predictable topologies, and tunable functionalities, it is predictable that COFs offer an ideal platform for adsorption, diffusion, and activation of CO_2 molecules. Besides this, COFs ensure the uniform distribution and binding of single metal active sites throughout their networks.[15] COFs have been employed in plentiful applications for instance sensors,[16] gas storage,[17] gas separation,[18] catalysis,[19] energy storage,[20] photo-energy conversion,[21] electronics and optoelectronics.[22] Researchers have focused on developing materials for photocatalysis and electrocatalysis, and in this regard, COF materials for energy conversion and energy storage are in high demand by converting solar energy into chemical energy and fuel cells.[23] Due to π-conjugation and coherent band structures, COF helps in light-

Surya Das

Ms Surya Das is currently a PhD student at the University of Kalyani. She received her master's degree in science also from the University of Kalyani. Her current research focuses on the development of porous materials for CO_2 reduction reactions and other organic transformations.

Sk. Manirul Islam

Prof. Sk. Manirul Islam obtained his PhD degree from the Indian Institute of Technology Kharagpur in 1999 and carried out postdoctoral research at the State University of New York, USA, during 2000–2001. At present, he is serving as a Professor of Chemistry at the University of Kalyani, West Bengal, India. The present thrust of his research is to design and synthesize functionalized porous materials, such as COFs, MOFs, POPs, and their catalytic applications towards CO_2 chemistry, CO_2 fixation to value-added chemicals, in situ transformation of CO, catalytic conversion of CO into value-added chemicals, biofuel synthesis, CC/CN bond formation reactions, and multicomponent coupling reactions.

harvesting, which promotes absorption and utilization of visible light during photocatalysis. Effective photo-induced charge carrier separation and transfer, which are crucial in photocatalysis, can be easily performed by adding functional groups to the skeletons of COFs. Additionally, to further improve the photocatalytic activity, COFs having a large surface area and suitable pore size can enhance mass transference and accommodate active molecules. COF-based materials for electrocatalysis can successfully resolve the conductivity and activity problems by adjustable molecular design and subsequent synthetic techniques where the building blocks can be connected *via* electron transmission channels, which can improve the efficiency of electrocatalysis. Also, electrocatalytic performances are enhanced by adding active sites, such as metal particles or functional groups to the COFs' frameworks. Therefore, crystalline COFs will be an idyllic model having outstanding potential for studying and understanding the highly effective electrocatalytic as well as photocatalytic CO_2 reduction.

1.1. Covalent organic frameworks

Covalent organic frameworks (COFs) are one of the categories of crystalline porous polymers where the monomer units are linked by strong covalent bonds. So, by varying the monomer units during their synthesis, COFs with desired functionalities, such as different dimensions and properties, can be obtained. COFs have gained huge attention from researchers all over the world since their first discovery by Yaghi and his research group in 2005.[11] The stability of COFs depends predominantly on the rigid covalent network of the systems. The arrangement and interaction between the layers of COFs are different for different dimensions. Thus, it is important for a researcher to understand the dimensions of the covalent organic framework. By understanding this, one can properly describe the properties of synthesized COFs. The dimensionality of COF depends on the geometry and connective patterns of the pioneers. Chemists have discovered the ability to form and control the covalent bonds in zero dimensions.[24] Further extension of the dimension of COFs from zero-dimensional to one dimension was made possible by the polymer chemists. Dimensionality influences a lot of the functionalities of COFs, which change from one dimension to the other.

• Topologically, covalent organic frameworks can be classified into 3 following categories.

1.1.1. One-dimensional COFs. One-dimensional (1D) COFs are mainly non-centrosymmetric linear crystalline polymers and can be synthesized by entropy-driven haphazard packing of organic chains, which mainly consist of one dimensionally-confined covalently bonded linkages, and mainly non-covalent interactions such as π–π interactions and hydrogen bonding. They show high degrees of freedom in molecular packing with enormously high anisotropy. A synthetic route for the preparation of novel 1D COF was recently depicted by Ziao Chen *et al.* with high surface area and thermal stability [Fig. 1b].[25] Recently, Hai-Sen Xu *et al.* also successfully discovered a strategy to construct 1D conjugated polymer and introduced labile metal to this polymeric system, they constructed single-crystal-metallo-

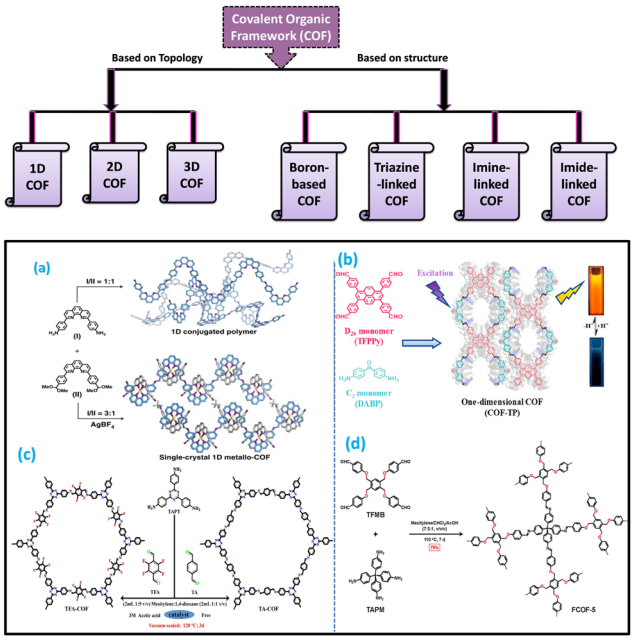

Fig. 1 Examples of the formation of covalent organic frameworks in different dimensions. The schematic diagram for the production of (a) and (b) 1D covalent organic framework, (c) 2D COF, and (d) 3D COF. Adapted with permission from ref. 26. Copyright © 2020, The Author(s); ref. 25. Copyright © 2020 American Chemical Society; ref. 37. © 2020 Elsevier B.V. All rights reserved; and ref. 47. Copyright © 2021 American Chemical Society.

COFs [Fig. 1a].[26] The linear chain of 1D COFs can also be transformed into 2D through chronological reversible-irreversible chemistries.[27] In recent times, Li and his group successfully constructed the heterojunction composite of 1D β keto-enamine-based COF/2D g-C_3N_4.[28] 1D COF/2D g-C_3N_4 acted as an efficient photocatalyst where the photocatalytic activity was basically enhanced due to visible-light adsorption capability of 1D β keto-enamine-based COF. Recently, Wang *et al.* constructed an ultrathin self-standing 1D COF nanofluidic membrane (denoted as BDA-TAM) having the ability to build an efficient nanofluidic osmotic energy generator.[29] As this, COF-based nanofluidic membrane, contains negative surface charges, it exhibits good selectivity towards cations and hence strong ionic conductance. Furthermore, the extraordinary stability of BDA-TAM extended across a wide range of saline solutions, temperatures, and pH values. This research broadens the area of utilization for self-standing 1D COF membranes, which can serve as a model for the fabrication of highly efficient osmotic energy generators.

1.1.2. Two-dimensional COFs. In 2014, the research group of Schlüter[30] and King[31] autonomously developed single crystals of 2D polymers. Two-dimensional COFs (2D COFs) consist of planar building blocks[32] where the planar sheets are generally arranged in a face-to-face direction and the strong interaction of π–π stacking present between contiguous layers present in 2D COF helps mobilize charge throughout the layers.[33] As such, it shows high electron delocalization and switchable band gap energy and that is why it plays a crucial role in electron conduction.[34] They are visible light responsive and show potential

applications in processes involving photocatalytic activity, *e.g.* H_2 evolution,[35] solar energy transformation, *etc.*[36] 2D COFs are highly crystalline, physically and thermally stable with high surface area porous polymers. In recent times, Yan *et al.* synthesized a newly designed fluorinated 2D COF having greater surface area and low band gap energy, which showed high photocatalytic activity towards H_2 evolution, in comparison with non-fluorinated COF [Fig. 1c].[37] Mateo-Alonso's group recently designed and synthesized a high π-stacking order and extremely crystalline wavy 2D COF (Marta-COF-2) and studied its structural properties to understand its charge transfer properties.[38] Marta-COF-2 was constructed using distinctly shaped monomers such as 2,3,10,11,18,19-hexahydroxy-catahexabenzocoronene (HBC) and benzene-1,4-diboronic acid (BDBA) using the so-called solvothermal method, which gives rise to wavy chair-like honeycomb lattice structure [Fig. 2(I)]. Besides this, recently, Zhao and his group explored a new simplistic way to synthesize 2D vinylene-based COFs (named, BTH-1, 2, 3) with electron-withdrawing benzobisthiazoles units through a versatile Knoevenagel polycondensation reaction.[39] Under this newly discovered reaction state, three novel completely sp^2-conjugated COFs having high BET surface areas (644, 686, and 1140 $m^2\ g^{-1}$ for BTH-1, BTH-2 and BTH-3, respectively) were constructed. These conjugated COFs served as acceptor moieties and showed semiconducting properties. It should be noted that under visible light irradiation, BTH-3 COF with electron-riched group benzotrithiophene demonstrated an impressive photocatalytic hydrogen evolution rate (HER), 15.1 mmol $h^{-1}\ g^{-1}$, which is significantly higher than those of BTH-1 (HER = 10.5 mmol $h^{-1}\ g^{-1}$) and BTH-2 (HER = 1.2 mmol $h^{-1}\ g^{-1}$), because of the prolonged π-conjugation and well-organized donor–acceptor (D–A) structure. This study first offers a simple method for developing sp^2-carbon conjugated COFs, secondly, the completely conjugated D–A type of COFs exhibit remarkable hydrogen evolution under the irradiation of light, which will unquestionably advance COFs in photocatalysis.

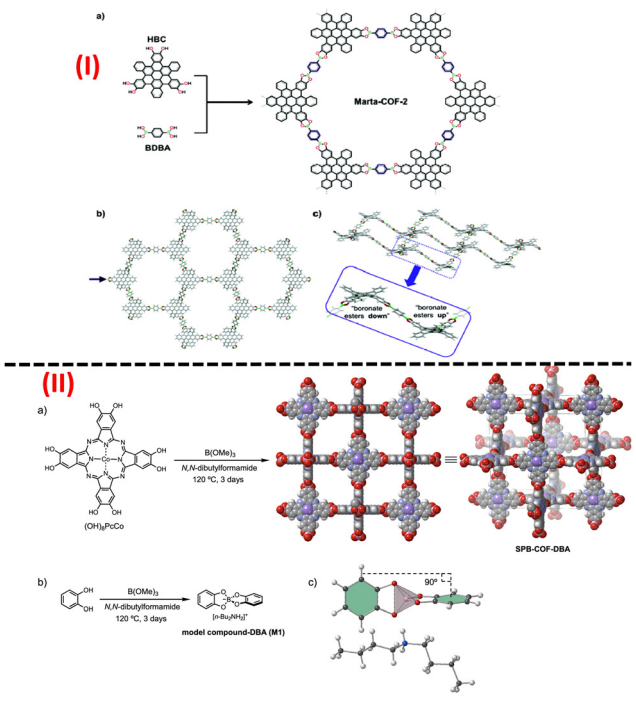

Fig. 2 A schematic representation of the formation of (I) wavy 2D COF and (II) cubic 3D COF. Adapted with permission from ref. 38. Copyright © 2021 Royal Society of Chemistry; ref. 48. Copyright © 2021 The Authors. Published by American Chemical Society.

1.1.3. Three-dimensional COFs. Three-dimensional (3D) COFs are periodic arrangements of tetrahedron building blocks.[40] In 3D COFs, molecular building units are arranged three-dimensionally into the framework, which facilitates open sites in COFs.[41] Noticeably, in comparison with 2D COFs, 3D COFs show much greater and highly accessible Brunauer–Emmett–Teller (BET) BET surface area, high crystallinity, thermal stability, a greater extent of active reaction sites, and photocatalytic activity, which has attracted a number of researchers recently. Based on these advantages, 3D COFs provide a significant advantages in gas storage and separation applications.[42] Recently, Wang's group developed bipyridine-linked 3D covalent organic frameworks (COFs) produced by using a mixture of tetrakis(4-aminophenyl)methane (TAPM), 2,2′-bipyridine-5,5′-diamine (Bpy), and 4,4′-biphenyldicarboxaldehyde (BPDA) using the solvothermal method.[43] Wang's research group depicted the preparation of 2D and 3D porphyrinic COF using same functional moieties and illustrated their different functionalities and properties and when compared with 2D porphyrinic COF, 3D COF showed better photocatalytic activity.[44] They also in recent times reported the synthesis of a switchable 3D COF, which showed a reversible transformation in the framework through redox path maintaining its crystallinity and porosity.[45] In recent times, 3D thioether-based covalent organic frameworks (JUC-570 and JUC-571) were developed by Zhang *et al.*, which showed high Hg^{2+} uptake capacity from water.[46] Recently, Wang's group reported the construction of a new highly crystalline porous 3D covalent organic framework (FCOF-5) by using flexible building blocks, which showed excellent breathing behavior, *i.e.*, upon adsorption/desorption of vapors can undergo reversible expansion/contraction [Fig. 1d].[47] Very recently, Cooper and his group developed a porous, crystalline and long-term ordered 3D COF (SPB-COF-DBA) by assembling simple and synthetically accessible square-planar cobalt(II) phthalocyanine (PcCo) units and tetrahedral spiroborate linkagesby[Fig. 2(II)].[48] The SPB-COF-DBA exhibited everlasting porosity having cubic pores with a higher BET surface area (1726 $m^2\ g^{-1}$). The majority of the reported lithium-ion-conducting COFs are 2D, in this regard, for the first time three kinds of poly(ethylene glycol) (PEG)-functionalized 3D COFs (3D-COF-PEG2, 3D-COF-PEG3 and 3D-COF-PEG6) with various lengths of PEG chains were effectively formed for ion transport in diverse directions by Zhang's group.[49] By incorporating LiTFSI into the COFs, 3D-COF-PEG2-Li, 3D-COF-PEG3-Li, and 3D-COF-PEG6-Li were synthesized. Because the combining actions of the fragment of the PEG chain and Li-ions are taken into account, the LiTFSI incorporated 3D COF attained a high ion conductivity of 3.6×10^4 S cm^{-1} at 260 °C, which demonstrates that PEG-based COFs are extremely safe as Li-ion polyelectrolytes at high temperatures. This research added a novel approach to the

development of highly effective PEG-based COFs for future-generation lithium-ion batteries.

• Based on structure, COFs are basically divided into the following four categories.

1.1.4. Boron-based COFs. Boron-based COFs are the first category of COFs which were initially synthesized by Yaghi and his groups in 2005.[11] COFs containing a huge number of B atoms are mainly constructed by boronate ester (C_2O_2B) or boroxine (B_3O_3) condensation. But these boron-containing COFs are not stable in moist air or in water and that is why their utility as a catalyst or for many long-standing uses became limited. Later, Zhang's group prepared boron-rich COFs having spiro-borate linkages, which displayed high thermal stability as well as hydrolytic and oxidative stabilities.[50] Boron-based COFs show strong Lewis acidity that facilitates N_2 adsorption.[51] Yan and co-worker showed that electrochemical excitation of boron-rich COFs led to the catalyst accessibility to N_2 and achieved NH_3 synthesis by reduction under ambient conditions.[52] Dong *et al.* reported porous boron-containing covalent organic frameworks, which exhibit strong ion adsorption ability and served as competent additives for Li^+ ion transference number improvement of the polymer electrolyte.[53] In recent times, Zhang's group prepared and immobilized Boron-based COF onto the surface of a capillary (COF-1@capillary column) and showed its application towards electro chromatographic separation [Fig. 3a].[54]

1.1.5. Triazine-based COFs. Covalent organic framework (COF) is fabricated from triazine or nitrile-containing starting material *via* the formation of covalent bonding.[55] 1,3,5-substituted triazine-based COF is more stable compared with the 1,3,5 substituted benzene-based COF because of the greater electron affinity of triazine than the benzene ring.[56] Chemically and thermally stable triazine-linked COFs show permanent tunable porosity, specific surface area, high N contents, high extraction efficiency towards some particular antibiotics, and also acts as an interesting adsorbents for organic pollutants[57] and excellent photocatalysts in many chemical reactions.[58]

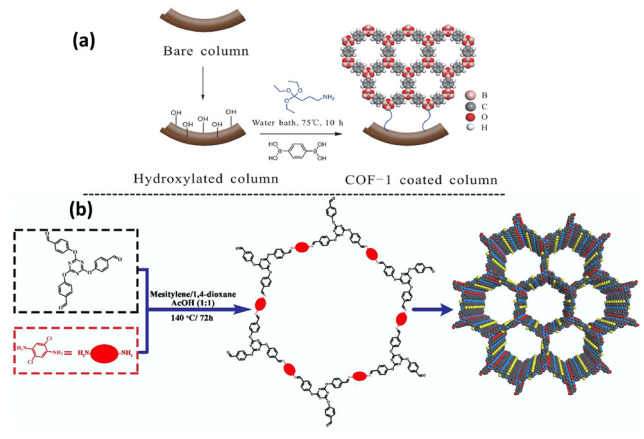

Fig. 3 A schematic diagram for the development of (a) Boron-based COF and (b) Triazine-based COF. Adapted with permission from ref. 54. Copyright © 2021 Elsevier B.V. All rights reserved; ref. 62. © 2021 Elsevier Ltd. All rights reserved.

In 2021, Dinari *et al.* effectively developed a triazine-based MIL-101-NH_2@COF for the elimination of dye-like acid blue 9 from the textile wastewater.[59] By incorporating 2,4,6-triphenyl-1,3,5-triazine, Dai *et al.* recently formed organic frameworks (COFs) and established them as excellent photocathodes for H_2 production.[60] This work demonstrates that the crystalline donor–acceptor COFs exhibited considerable applications towards water splitting as highly efficient organic photoelectrodes. In 2020, Afshari *et al.* synthesized a novel porous triazine ring-based nanoneedle T-COF through a facile one-pot hydrothermal reaction, which showed super absorptivity (adsorption capacity of 1826 mg g^{-1}), for the removal of the heavy metal ion Hg^{2+} from aqueous solutions[61] and after that in recent times they also adopted a triazine-linked FT-COF *via* the solvothermal method to prosper the fire protection and mechanical characteristics of thermoplastic polyurethane (TPU) [Fig. 3b].[62] In 2022, among the porous triazine COFs, COF (TS-COF) was synthesized and reported by Wang *et al.* employing the condensation of monomer units 1,3,5-tris-(4-aminophenyl)triazine (TAPT) and squaric acid (SA) under the solvothermal process. To study the electrochemical activity, Au nanoparticles were incorporated at the surface of TS-COF to develop AuNPs@TS-COF composite and further modification was carried out to constructAuNPs@TS-COF/RGO/GCE.[63] It was found that the electrochemical performance was greatly enhanced from TS-COF to AuNPs@TS-COF and then to AuNPs@TS-COF/RGO/GCE as the electrochemical sensors and this opened a new way to use triazine-based COF for designing electrochemical sensors. At the same time, Kim *et al.* fabricated a rigid and planar triazine-based Covalent Organic Frameworks (TACOF1) by assembling the starting materials, 2,4,6-tris(4-formylphenyl)-1,3,5-triazine (TFPT) and hydrazine monohydrate.[64] By direct carbonization of TACOF1 in a nitrogen atmosphere, they formed nitrogen-doped nanoporous carbon that contained a high surface area (1194 m^2 g^{-1}). The carbonized TACOF1 formed at 800 °C showed good capacitive ability owing to its nitrogen-riched porous framework structures. Liang *et al.* designed and prepared triazine-based porous crystalline covalent organic framework COF-SQ, which was further functionalized to generate quinoline-linked COF termed COF-SQ-Ph.[65] Functionalized COF-SQ-Ph acted as a promising recipient and storage of sulphur and are being used as electrode materials in Li–S batteries due to their unique extended π-conjugated network. This study also promotes the large-scale synthesis of functionalized triazine-based COF material. Meanwhile, Zhang's group showed the application of allyl-riched COF (ART-COF) as a cathode host material for Li–S batteries.[66] These studies suggested a reasonable approach toward the development of exceedingly stable and long-lasting Li–S batteries. Recently, the development of porous and highly efficient covalent organic frameworks (COFs) with large surface areas and low band gap energy have been achieved using the so-called solvothermal methodology by Liu's group.[67] The synthesized COFs (designated as TTA-TTB and TAPB-TTB) possess donor–acceptor properties and thus serve as outstanding photo-cathodes for the production of H_2 without using any sacrificial electron donor or cocatalyst. It was noticed that TAPB-TTB COF (110 A cm^2) exhibit suggestively better visible-light-induced photocurrent responses compared to TTA-TTB COF (35 A cm^2).

1.1.6. Imide-based COF. Imide-linked COFs were first reported by Yan and his co-workers in 2014 through the imidization reaction [18]. Imide-based COF materials with their high-performance aromatic frameworks provide high thermal stability as well as high porosity and surface area and they exhibit wide applications in packing dye molecules and deliver drugs,[68] energy storage,[69] photocatalysis,[70] *etc.*

Recently, Nagai and his research group proposed a synthesis route of four redox-active mesoporous polyimide (PI) based COFs [Fig. 4a].[71] DFT study and XRD analysis of the synthesized COFs revealed that the imide bonds form at an angle with one another, which minimizes the pore width and extends the pore walls. Recently, under a high-temperature solvothermal method, highly crystalline 2D imine-based COF was achieved with uniform porosity by Liu and co-workers.[72] In this work, COF was used as a support for Ru^{3+} and the Cryst-2D-PMPI-Ru exhibited high electrocatalytic performance and stability. Recently, Zhao *et al.* reported the construction of two polyimide-based covalent organic frameworks in a green way without using any organic solvent and both COF (COF-1 and COF-2) showed outstanding fluorescence sensing properties for a variety of metal ions and distinctive antibiotics.[73] Liu's group recently reported a 2D polyimide-based COF (PI-NT COF), which was prepared *via* a simplistic optimized solvothermal process on indium tin oxide-coated glass substrate.[74] This PI-NT COF exhibited highly ordered crystalline, tunable thickness, and smooth surface, and owing to the inherent charge-transfer properties of 2D COF films, it showed excellent potential in high-performance data storage devices with low inaccuracy, high conformity, and stability. Maschita *et al.* proposed a new path for the synthesis of polyimide-linked COFs in 2020.[75] In this work, they developed crystalline and porous COFs *via* the ionothermal process in $ZnCl_2$ and eutectic salt mixtures and this method diminished the reaction time surprisingly compared to that of a typical solvothermal process and occurred without using any environmentally harmful solvents or catalyst. Recently, Maschita *et al.* prepared a series of stable, long-range crystalline porous imide-linked covalent organic frameworks (TAPA-PMDA-COF, TAPB PMDA-COF, and TAPE-PMDA-COF) following a green environmentally friendly approach using alcohol-supported hydrothermal polymerization method (aaHTP) permitted to obtain a new class of imide-based COFs by avoiding the toxic solvents.[76] Synthesis of imide-linked TAPA-PMDA-COF, TAPB PMDA-COF, and TAPE-PMDA-COF was formed by the transformation of imine-linked COFs *via* linkage substitution. Additionally, Kim's group successfully synthesized porous crystalline polyimide-linked COFs (PICs) *via* geomimetic hydrothermal reaction conditions. They also established that the PICs possessed exceptional redox-active properties along with high surface area and served as a promising anode material in Li-ion batteries.[77]

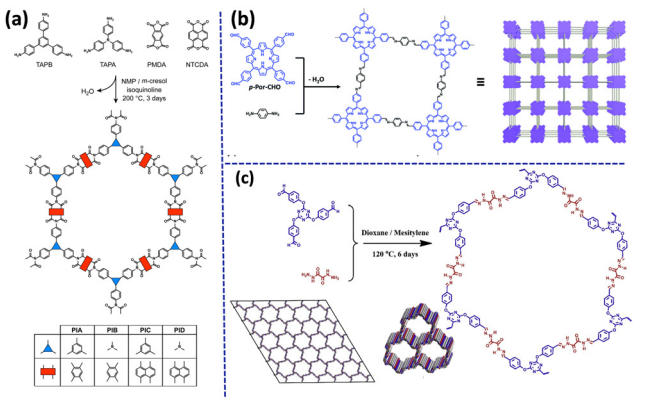

Fig. 4 Schematic route of preparation of (a) polyimide-based COFs, (b) porphyrin-based imine-linked COF and (c) hydrazone-based imine-linked COF. Adapted with permission from ref. 71. Copyright © 2021 American Chemical Society; ref. 83. Copyright © 2021 Royal Society of Chemistry; ref. 87. © 2020 Elsevier B.V. All rights reserved.

1.1.7. Imine-linked COF. In 2009, Yaghi and co-workers successfully constructed a different class of covalent organic framework based on the dynamic covalent chemistry that mainly contained distinct –C═N– bonds and acquired 3D five-fold interpenetrating diamond-like structure.[78] Presently, the synthesis of imine-based COFs can be divided into two groups. One method is a condensation reaction between aldehyde and amine *i.e.*, the Schiff base type of reaction[79] and the other is a co-condensation reaction between an aldehyde and hydrazides.[80] In other words, imine-based COFs gain much better crystallinity and structural regularity in comparison with other COFs as well as they possess much higher thermal and chemical stability compared to boron-based COFs. Also, 2D porous imine-linked COF membranes performed well in the C_2H_6/CH_4 separation with high selectivity.[81] Recently, Zamora and co-workers demonstrated a three-step process to prepare 2D imine-based COF aerogels having low densities and excellent porosities and showing outstanding adsorption capability.[82]

The study of the photocatalytic behavior of 2D imine-linked COFs has recently attracted much attention from researchers. Feng *et al.* reported the photocatalytic activity of porphyrin-based imine-linked COF (Por-COF) in the presence of (2,2,6,6-tetramethylpiperidin-1-yl)oxyl (TEMPO) [Fig. 4b].[83] It was found that the presence of TEMPO enhanced the photocatalytic efficiency of Por-COF in the aerobic oxidation of sulfides selectively under visible light irradiation because of the supportive photocatalysis amongst Por-COF and the redox mediator, TEMPO. In the report of Chen's group, a porphyrin-based imine-linked covalent organic framework (TPE-Por-4) was constructed successfully by the condensation of the 5,10,15,20-tetra-(4-aminophenyl) porphyrin (Por-4) and 4,4′,4″,4‴-(ethane-1,1,2,2-tetrayl) tetrabenzaldehyde (TPE) monomers following solvothermal conditions.[84] The suspension of the TPE-Por-4 exhibited exceptional fluorescence properties and a noticeable response to pH variations, ordering from 2 to 4 was observed. Imine-based covalent organic frameworks can act as a support material for metal ions through 'N' and 'O' sites present in it and the formed 'metal ion-based COF' can provide catalytic activity for a selective organic transformation. Gao's group recently developed Cu(I)-immobilized-COF TpBpy-Cu) wherein TpBpy is an imine-linked porous COF containing N, N, and N, O chelating sites.[85] Cu(I)-TpBpyCOF proved to be an efficient catalyst because of the synergy effect between COF and Cu(I) sites for the terminal alkyne carboxylation

reaction under 1 atmosphere of CO_2 pressure and 60 °C. Four isostructural porphyrinic 2D COFs were constructed and characterized and their photocatalytic activity for H_2 production from water was determined by Chen *et al.*[86] Further, by the amalgamation of different metal ions at the surface of the COF's porphyrin units, photophysical and electronics properties of the COFs can be adjusted.

Hydrazone-linked COFs show structural variety, are synthetically accessible and extremely high thermal and chemical stability, and contain a copious number of N atoms, which facilitates the adsorption of gas molecules. A recent report by Amini and co-workers provided a synthetic route for the formation of hydrazone-based 2D COF by a condensation reaction between 2,4,6-tris(*p*-formylphenoxy)-1,3,5-triazine and oxalyl dihydrazide under the solvothermal approach [Fig. 4c].[87] This obtained imine-linked hydrazone-based COF was highly stable in boiling water or even in a strongly acidic medium and provides a large BET surface area with high CO_2 uptake ability. Recently, Ahmed *et al.* illustrated the construction of a novel hydrazone based highly crystalline, and chemically stable covalent organic framework (TFPB–DHTH COF) *via* solvothermal analysis using 1,3,5-tris(4-formylphenyl)benzene (TFPB) and 2,5-dihydroxyterephthalohydrazide (DHTH) as starting materials.[88] Recently, Zhang and co-workers similarly established the synthesis of a new stable covalent organic framework (Tfpa–Mth COF) *via* the condensation (Schiff base) reaction involving tris(4-formylphenyl) amine (Tfpa) and a chiral hydrazide (Mth).[89] Tfpa–Mth COF achieved fluorescence property due to its uniformly distributed surface and thick films and acted as a potential fluorescent sensor for the recognition of Fe (III) ions. A recent finding from S. Wu *et al.* showed that a well-ordered two-dimensional hydrazone-linked crystalline porphyrinic COF, Por-DETH-COF, was congregated from 5,10,15,20-tetrakis (4-benzaldehyde) porphyrin (*p*-Por-CHO) and 2,5-diethoxyterephthalohydrazide (DETH), followed by a study of its excellent photocatalytic activity assessed with the oxidation of benzyl amines to the selectively for imines in the presence of air and red-light irradiation.[90] Along this line C. Zhang, Y. Dong, and co-workers utilized a quintessential bicarbazoleusing as the major building block units and hydrazone as the linkers to synthesize a 2D COF (CZ-DHZ-COF) and showed that CZ-DHZ-COF generates intense cyan colour emission in its solid state.[91] The as-synthesized powder-like CZ-DHZ-COF exhibited fast fluorescence response with weak and red-shifted fluorescence towards acid vapor; besides this, the liquid obtained by suspending CZ-DHZ-COF showed precise identification for Fe(III) ions with excellent fluorescence quenching. Hence, CZ-DHZ-COF would act as a decent applicant for fluorescence sensing to distinguish Fe(III) ions and acid vapor, also used in versatile applications for fluorescence sensing.

Amide-based COFs show vast potential in diverse practical applications because of their high stability and crystallinity of the porous polyamide structural moiety. But due to the lack of proper synthetic approaches, very few amide-linked COFs have been reported till now. Yaghi and his co-workers, first in 2016, reported two amide-based COFs *via* the oxidation of the imine linkages of the imine-based COF using an oxidizing agent, sodium chlorite.[92] Just a while ago, similar to that one reported by Yaghi's group, amide-linked highly porous crystalline COF was synthesized using $KHSO_3$ as an oxidant by rapid conversion from the imine-linked framework into amide-linked framework under green reaction condition.[93] Later in 2020, Yan's group designed and constructed an irreversible amine-based COF termed as JNU-1, which exhibited good stability, excellent selectivity, extraordinary fast kinetics and high-absorbance capacity for gold recovery.[94] The building block exchange (BBE) tactic was involved for the construction of JNU-1 COF. Due to its intrinsic linkage and the presence of functional groups, COF is irreversible and hence leads to the ultrafast recovery of gold selectively. Far ahead, Yang and his group synthesized a novel 2D amide-linked covalent organic framework (COF-TM), wherein COF acted as a support for Pd(II) ion in Pd@COF-TM.[95] The synthesized Pd@COF-TM showed outstanding catalytic activity for Suzuki-Miyaura coupling reaction, it also was demonstrated that the heterogeneous catalyst Pd@COF-TM exhibited high durability and high recyclability up to nine consecutive cycles. In recent times, Ma *et al.* synthesized amide-linked 2D COF (COF-JLU19) with electron donor-acceptor structural properties with inherent porosity, high specific BET surface area, good stability along with brilliant photoelectric property [Fig. 5(I)].[96] COF-JLU19 showed excellent photocatalytic activity and good recyclability using water as a medium under metal-free conditions and visible light irradiation. They also prepared an amide-linked COF-JLU19 electrospinning membrane and photocatalytic activity with recyclability towards the photodegradation action of

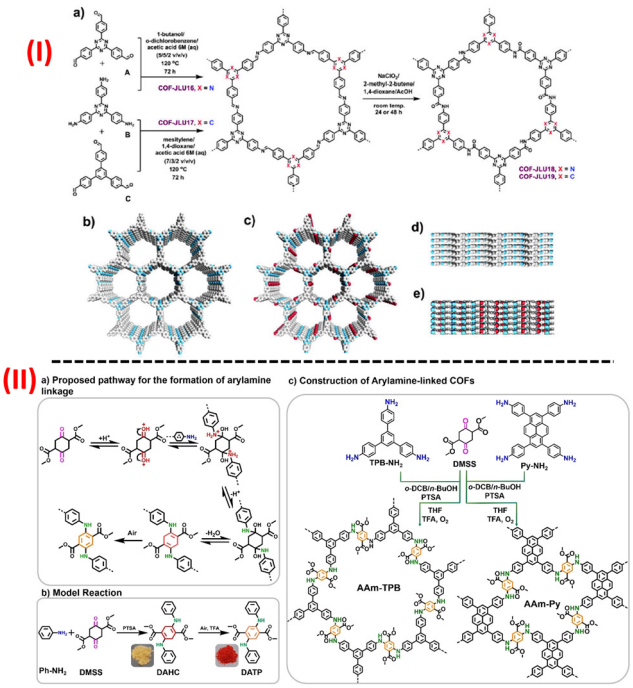

Fig. 5 A schematic representation for the construction of (I) amide-based COFs, (II) aryl amine-based imine-linked COF. Adapted with permission from ref. 96. Copyright © 2021 Dalian Institute of Chemical Physics, the Chinese Academy of Sciences. Published by Elsevier B.V. All rights reserved; ref. 99. © 2021 Wiley-VCH GmbH.

Rhodamine B (RhB) in H_2O under sunlight irradiation was studied. Das *et al.* recently applied the strategy of incorporating new functional groups like amide and hydrazide into the COF material in order to improve their porosity, stability, and crystallinity by the formation of inter and intralayer H-bonding.[97] Thus, they effectively constructed three triazine-based amide-hydrazide linked COFs named as CON, CONN, and CONNCO and also showed that these COFs have luminescent properties with fascinating fluorescence on-off different pH-responsive for scavenging of protons from an aqueous solution.

Again, another triazine-based two new photoactive 2D COFs of imine and amide-linkages (COF-JLU32 and COF-JLU33) have been recently reported by Liu's group and their photocatalytic experiment for the preparation of α-trifluoromethylated ketones was tested.[98] Mainly, amide-linked COF-JLU33, a metal-free catalyst, exhibited efficient photocatalytic activity as well as good recyclability related to the other reported heterogeneous catalysts.

For the first time, Chen and his group recently evaluated an efficient strategy to develop a new aryl amine-linkage for the synthesis of COFs, which enriched the COFs with other tailored characteristics along with the present building blocks, and thus modified the COFs with required functions [Fig. 5b].[99] The group successfully prepared two aryl-linked COFS AAm-TPB and AAm-Py having hcb and sql topologies, respectively, with better stability as well as a highly conjugated network and they also explored their pseudocapacitive energy storage capacity and AAm-TPB COF exceptionally exhibited the highest capacitance of 271 F g^{-1} among the other reported COF-based electrode material.

The variation in physical properties with the structure of the COF is illustrated in Table 1, from which we can observe that using triazine as a monomer unit, the textural property of the COF is enhanced. Moreover, due to the presence of more N atoms in the structure, it has been established that highly polar and N-rich Lewis-base groups can facilitate the adsorption and activation of carbon dioxide. On the other hand, from Table 2, it is easy to notice that the majority of reports found in the literature dedicated to COF-based catalytic CO2RR are based on the formation of hybrid materials in which the semiconductor COF is combined with a different metal or other conductive materials. As a result, fine-tuning of various parameters like appropriate monomer units for the hybrid materials, the physical hetero-junction created between both hybrid materials, relative molar ratios, or the specific location of the dopant onto the catalyst, involved in the formation of a heterogeneous nanohybrid, could have an impact on the electronic structure of the COF and also on its active sites and thus different catalytic properties of the materials has been noticed.

Table 1 Relationship between structure and physical properties of COFs

Type of COF	Monomer units	Synthesis process	Physical properties	Ref.
Boron based COFs	1,4-Benzene diboronic acid (BDBA)	Static solvothermal method	S-COF-1: S_{BET} = 690 m^2 g^{-1}, V_{total} = 0.47 cm^3 g^{-1}	53
		Solvothermal method	H-COF-1@5: S_{BET} = 717 m^2 g^{-1}, V_{total} = 0.46 cm^3 g^{-1} H-COF-1@10: S_{BET} = 812 m^2 g^{-1}, V_{total} = 0.48 cm^3 g^{-1} Ionic conductivity (H-COF-1@10 > H-COF-1@5 > S-COF-1) Crystallinity (S-COF-1 > H-COF-1@5 > H-COF-1@10)	
Triazine-based COFs	4,4′,4″-(1,3,5-triazine-2,4,6-triyl)trianiline (TTA) and 4,4′,4″-(1,3,5-triazine-2,4,6-triyl)tribenzaldehyde (TTB)	Solvothermal method	TTA-TTB COF: S_{BET} = 1592 m^2 g^{-1}, pore size = 2.2 nm, V_{total} = 1.08 cm^3 g^{-1}, band gap = 2.67 eV	67
	1,3,5-tris(4-aminophenyl)benzene (TAPB) and 4,4′,4″-(1,3,5-triazine-2,4,6-triyl)tribenzaldehyde (TTB)	Solvothermal method	TAPB-TTB COF: S_{BET} = 932 m^2 g^{-1}, pore size = 2.19 nm, V_{total} = 0.65 cm^3 g^{-1}, band gap = 2.43 eV	
Imidebased COF	2,4,6-tris(4-aminophenyl)-benzene (TAPB) and perylene-3,4,9,10-tetracarboxylic dianhydride (PTCDA)	Ionothermal method	TAPB-PTCDA-COF: S_{BET} = 1250 m^2 g^{-1}, Pore width = 31 Å, highly crystalline	75
	2,4,6-tris(4-aminophenyl)-benzene (TAPB) and pyromellitic dianhydride (PMDA)	Ionothermal method	TAPB-PMDA-COF: S_{BET} = 460 m^2 g^{-1}, pore width = 29 Å, highly crystalline	
Imine linked COF	1,3,5-triformylphloroglucinol (Tp) and 2,2′-bipyridine-5,5′-diamine (Bpyda)	Solvothermal method	TpBpy: S_{BET} = 1480 m^2 g^{-1}, CO_2 adsorption capacity = 66.8 cm^3 g^{-1} TpBpy-Cu: S_{BET} = 460 m^2 g^{-1}, CO_2 adsorption capacity = 47.2 cm^3 g^{-1} Crystallinity (TpBpy > TpBpy-Cu)	85
Hydrazone-linked COF	2,4,6-tris(*p*-formylphenoxy)-1,3,5-triazine and oxalyl dihydrazide	Solvothermal method	TPT/OH COF: S_{BET} = 424 m^2 g^{-1}, CO_2 capture capacity = 0.9 mmol g^{-1}, highly chemically stable	87
Triazine-based imine linked COFs	1,3,5-tris-(4-aminophenyl)triazine (TAPT) and benzo[1,2-*b*:3,4-*b*′:5,6-*b*″]trithiophene-2,5,8-tricarbaldehyde (BTT)	Solvothermal method	COF-JLU32: S_{BET} = 1501 m^2 g^{-1}, V_{total} = 0.707 cm^3 g^{-1}, highly crystalline, optical band gap energy (E_g) = 2.46 eV	98
Triazine-based amide linked COFs	TPT/OH COF (imine-linked COF)	Irreversible conversion from the imine-linked framework into an amide-linked framework	COF-JLU33: S_{BET} = 1148 m^2 g^{-1}, V_{total} = 0.701 cm^3 g^{-1}, highly crystalline, optical band gap energy (E_g) = 2.37 eV Crystallinity (COF-JLU 33 > COF-JLU32)	98

Table 2 COFs and their composites for CO_2 reduction

Catalyst	Surface area ($m^2\ g^{-1}$)	Process	Product	Yield	Ref.
COF	432	Photo-reduction	Carbon monoxide (CO)	18.7 (TON)	102
COF	521	Photo-reduction	CO & O_2 (trace amount CH_4, H_2)	102.7 mol g^{-1} h^{-1} (CO) & 51.3 μmol g^{-1} h^{-1} (O_2)	103
COF	421.64	Photo-reduction	HCOOH and HCHO	0.027 mole HCOOH, 0.96 mole HCHO	104
COF	571.6	Photo-reduction	CO	54 (TON)/17.93 mmol g^{-1}	105
COF	843.8	Photo-reduction	CO, H_2, O_2	295.2 μmol g^{-1}	106
DQTP COF-Co	195.92	Photo-reduction	CO	1.02 × 103 μmol h^{-1} g^{-1}	107
DQTP COF-Zn	345.57	Photo-reduction	HCOOH	152.5 μmol h^{-1} g^{-1}	107
COF/[Ir-ppy]	137.9	Photo-reduction	CO	88.6 μmol h^{-1} g^{-1}	108
Re-Bpy-sp2c-COF	323	Photo-reduction	CO	1400 mmol g^{-1} h^{-1}	109
PdIn@N3-COF	100.46	Photo-reduction	MeOH (74%), CH_3CH_2OH (26%)	798 μmol g^{-1}	110
COF-3	1010	Photo-reduction	Formic acid (HCOOH)	170 μmol	111
COF-4	1660	Photo-reduction	HCOOH	226.3 μmol	111
3.0 wt.% Ru/TpPa-1	385	Photo-reduction	Formic acid (HCOOH)	108.8 μmol g^{-1} h^{-1}	112
TpBD-H_2	535	Photo-reduction	Formic acid (HCOOH)	45.7 μmol g^{-1} h^{-1}	113
TpBD-$(CH_3)_2$	406	Photo-reduction	Formic acid (HCOOH)	86.3 μmol g^{-1} h^{-1}	113
TpBD-$(OCH_3)_2$	388	Photo-reduction	Formic acid (HCOOH)	108.3 μmol g^{-1} h^{-1}	113
TpBD-$(NO_2)_2$	259	Photo-reduction	Formic acid (HCOOH)	22.2 μmol g^{-1} h^{-1}	113
COF-TVBT-PA	198.4	Photo-reduction	CO	70.8 μmol g^{-1}	114
COFbpyMn	1601	Electro-reduction	Carbon monoxide (CO)	TON = 5800	115
Co-mNC_{COF}	1985	Electro-reduction	Carbon monoxide (CO)	FE_{CO} = 81%	116
Fe-mNC_{COF}	—	Electro-reduction	CO	FE_{CO} = >90%	116
Ni-mNCCOF	—	Electro-reduction	CO	FE_{CO} = >95%	116
AAn-COF-Cu (NF)	161	Electro-reduction	CH_4	FE_{CH_4} = 77%	117
OH-AAn-COF-Cu (HT)	470	Electro-reduction	CH_4	FE_{CH_4} = 61%	117
2D TT-Por(Co)-COF	748	Electro-reduction	CO	FE_{CO} = 91.4%	118
NiPc-COF	358	Electro-reduction	CO	FE_{CO} = 99.1%	119
TTF-Por(Co)-COF	888	Electro-reduction	CO	FE_{CO} = 95%	120
Co-TTCOF	481	Electro-reduction	CO	FE_{CO} = 99.7%	121
CoPc-PI-COF-1	181	Electro-reduction	CO	FE_{CO} = 97%	122
CoPc-PI-COF-2	291	Electro-reduction	CO	FE_{CO} = 96%	122
TAPP(Co)-B18C6-COF	942	Electro-reduction	CO	FE_{CO} = 93.3% TOF = 1267 h^{-1}	123
TAPP(H2)-B18C6- COF	906	Electro-reduction	CO	FE_{CO} = 86%	123
CoPc-PDQ-COF	762	Electro-reduction	CO	TOF= 11 412 h^{-1}	124
COF-366-$(OMe)_2$Co@CNT	196	Electro-reduction	CO	FE_{CO} = 93.6%	125
NiPc/CoPc-TFPN COF	252.375	Electro-reduction	CO	FE_{CO} = 99.8%	126
NiPc/CoPc-TFPN COF	252.375	Photo-electroreduction	CO	FE_{CO} ~ 100%	126
Cu@[OH]-H_2P-COF/CF	895	Photo-electroreduction	CH_3OH, CH_3CH_2OH, CH_3OCH_3, $CH_3CH(OH)_2$	5352 μM g^{-1} h^{-1}	127
NAHN-Tp	137.9	Photo-reduction	CO	88.6 μmol h^{-1}	128
CoPc-PI-COF-1	181	Electro-reduction	CO	FE_{CO} = 97%	129
CoPc-PI-COF-1	291	Electro-reduction	CO	FE_{CO} = 96%	129
CoPc-PI-COF-3	415	Electro-reduction	CO	FE_{CO} = 96%	130
H_2Pc-PI-COF-3	320	Electro-reduction	CO	FE_{CO} = 21%	130
3D-Por (Co/H)-COF	922	Electro-reduction	CO	FE_{CO} = 92.4% TOF = 4610 h^{-1}	131
Re-TpBpy	—	Photo-reduction	CO	19.6 μmol g^{-1} h^{-1}	132
MWCNT-Por-COF-Co	—	Electro-reduction	CO	FE_{CO} = 99.3%	133
MWCNT-Por-COF-Cu	—	Electro-reduction	CH_4	FE_{CH_4} = 71.2%	134

2. Application

2.1. CO_2 reduction

The reactions involved in the CO_2 reduction process are shown below:

$$CO_2 + 2H^+ + 2e^- \rightarrow HCOOH$$

$$CO_2 + 2H^+ + 2e^- \rightarrow CO + H_2O$$

$$CO_2 + 4H^+ + 4e^- \rightarrow C + 2H_2O$$

$$CO_2 + 4H^+ + 4e^- \rightarrow HCHO + H_2O$$

$$CO_2 + 6H^+ + 6e^- \rightarrow CH_3OH + H_2O$$

$$CO_2 + 8H^+ + 8e^- \rightarrow CH_4 + 2H_2O$$

$$2CO_2 + 8H_2O + 12e^- \rightarrow C_2H_4 + 12OH^-$$

$$2CO_2 + 9H_2O + 12e^- \rightarrow C_2H_5OH + 12OH^-$$

2.1.1. Electrocatalytic CO_2 reduction (ECR). The electroreduction of CO_2 using different types of COF catalysts is shown in Table 2. Generally, a wide range of metal particles and metal oxide-based catalysts are used for the reduction of carbon dioxide.[100] Electrochemical Reduction of CO_2 using heterogeneous solid catalysts is affected by the interaction between the adsorbed CO_2 molecule at the surface of catalysts, electrons, and protons. Mainly three fundamental steps are involved in

the electro-catalytic CO_2 reduction reaction: (i) CO_2 molecule adsorption at the surface of catalyst; (ii) sharing of electron and proton between catalyst and CO_2; (iii) the desorption of products (Fig. 6). The first step is the most crucial step for operating the whole reaction and achieving products. By sharing electrons, CO_2 is transformed into $CO_2^{\cdot-}$ radical anion species. Depending on the type of the catalyst, different types of reaction pathways or grouping of two or more reaction steps can lead to the formation of a wide range of products by CO_2 reduction. Electrochemical reactions occur in the liquid phase, so protons remain free to react. If the catalyst has a weak capability of absorbing CO intermediate, then CO is obtained as a major product *via* the formation of the COOH* intermediate followed by the addition of one electron and proton. Catalysts with pi electrons can improve the absorption of $CO_2^{\bullet-}$ radical and thus inhibit further reduction of $CO_2^{\bullet-}$, consequential in the formation of formate through the protonation method. The production of the liquid fuel CH_3OH is mainly achieved *via* the CH_3O intermediate from CO_2 followed by protonation. Under the electrochemical environment dimerization of two carbon radical anions give rise to the synthesis of C_2 products (such as C_2H_4, and C_2H_5OH). The production of hydrocarbons, as well as CH_4 and C_2H_4, is achieved due to the transformation of the adsorbed CO to *CHO *via* the hydrogenation process and further hydrogenation is not possible because CHOH is thermodynamically unstable.[101] Formations of CH_4 from CO_2 are generally 8 electron processes and occur at high potential. Therefore, a variety of side products *e.g.*, ethane, hydrogen, CO, formate, *etc.* are obtained because of the applied high potential, and thus selectivity of CH_4 synthesis becomes low. From Table 2, based on the reported literature, it is observed that metal-based (*e.g.*, Fe, Cu, and Co) COFs are more efficient for the electrocatalytic reduction of CO_2, and selectively CH_4 or CO is obtained as a product, *i.e.*, the efficiency of electrocatalytic reactions is increased significantly in the presence of metal particles.

2.1.2. Photocatalytic CO_2 reduction (PCR). The photoreduction of CO_2 involving a variety of COF-based catalysts is illustrated in Table 2, from which it can be observed that the noble metal Re-complex combined with COF materials proved to be an excellent photocatalyst and exhibited outstanding efficiency in the photocatalytic reduction of CO_2. Re-Bpy-sp2c-COF catalyst prepared by Cooper's group in 2019, showed 1400 mmol g^{-1} h^{-1} CO production from CO_2 with up to 86% selectivity.[109] They demonstrated that tethering molecular catalysts—a complex of rhenium, $[Re(bpy)(CO)_3Cl]$ along with a crystalline covalent organic framework (COF) offered a heterogeneous photocatalyst, which exhibited strong absorption of light in the visible region, a high-affinity CO_2-binding and eventually an enhanced catalytic performance beyond its homogeneous Re counterpart. The bipyridine sites on the COF permitted the Re complex to be ligated into a completely p-conjugated backbone, which is chemically stable and promotes light harvesting.

For the photocatalytic reduction of CO_2, metal-impregnated COF-based materials and hybrid COF catalyst systems coupled with homogeneous metal-complex possess better activity compared to pure COFs. This activity enrichment was mainly endorsed by the presence of transition-metal elements, which usually facilitate excellent CO_2 adsorption with high-catalytic capability or have the capacity to significantly intensify photo-induced charge generation and enhance the charge-transfer process. It is noticeable from the preceding existing literature, that both only COF and metal-based COFs are reported for the reduction of CO_2 to C_1 as well as C_2 products based on the physical and chemical properties of different types of COFs (Table 2).

In 2019, the group created the world's first metalated COF material for heterogeneous photocatalytic CO_2 reduction.[107] DMA (*N*,*N*-dimethylacetamide)/1,3,5-trimethylbenze/acetic acid mixed solvent was mixed with 2,6-diaminoanthraquinone (DQ) and 2,4,6-triformylphloroglucinol (TP), which was then heated at 120 °C/72 h. CO and HCOOH were synthesized using the metalated COFs. Fig. 7 depicts the reaction mechanism schematically. Metal coordinating sites *via* anthraquinone O atoms were abundant in the as-prepared 2D-anthraquinone-based DQTP-COF. To incorporate the Co(II) ion into the COF structure, the aqueous solution was sonicated, followed by heating with cobalt salt. Under visible-light irradiation ($\lambda \geq 420$ nm) sensitized by Ru(II) salt and employing TEOA as a sacrificial electron donor, the as-prepared DQTP-COF-Co catalyst demonstrated promising CO_2 reduction capability. The as-prepared metalated catalyst produced CO at a rate of 1.02×10^3 μmol g^{-1} h^{-1}, which was significantly greater than non-metalated DQTP-COF, DQTP-Ni-COF, and DQTP-Zn-COF samples. CO had moderate selectivity over H_2 (59.4 percent). When the Zn(II) ion was loaded into the DQTP-COF structure, however, HCOOH was produced with a selectivity of up to 90% and a formation rate of 152.5 μmol g^{-1} h^{-1}. For this distinguishing selectivity, the scientists postulated a ''two-pathway'' mechanism. The two pathways forming either HCOOH or CO share the same intermediate, *i.e.*, M-COOH. When the coordination environment for COOH was electron-rich, the C–O bond was prone to cleavage, forming CO product, whereas when the coordination environment was electron-deficient, HCOOH formation was facilitated *via* the proton-coupled-electron-transfer process (PCET), which bypassed the C–O cleavage pathway. CO was the predominant product because CO is an excellent-electron donor, whereas the – electron acceptor metal centre in Zn-based COF would encourage the synthesis of HCOOH. The generation rates of CO and HCOOH were nearly comparable for Ni-COF, which was neither electron-rich nor deficient. Lan's research was the first to use metalated-COF as a heterogeneous photocatalyst for the reduction of CO_2.

Huang *et al.* applied a viable strategy for the conversion of CO_2 into C_1/C_2 alcohols, expanding the field of artificial photosynthesis.[110] Different composites of PdxIny@N3-COF where x:y = 1:0, 0:1, 1:2, 1:1, 2:1 were easily constructed using bimetallic PdIn nanoclusters enclosed in a photoactive COF (N3-COF). The resultant PdIn@N3-COF showed remarkable photoactivity for CO_2 reduction along with H_2O oxidation into

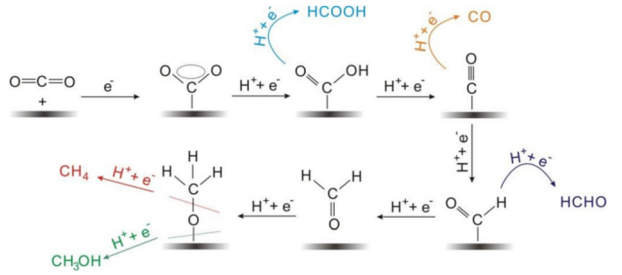

Fig. 6 The proposed reaction mechanism of production of mainly C_1 products by electrochemical CO_2 reduction. Adapted from ref. 100. © 2017 Wiley-VCH Verlag GmbH & Co. KGaA, Weinheim.

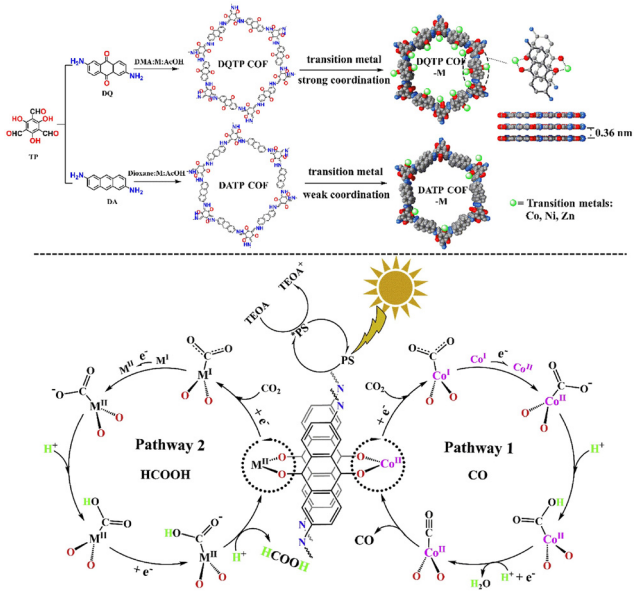

Fig. 7 Synthesis and metallization process of DQTP COF and DATP COF and proposed mechanism for the photocatalytic reduction of CO_2 with DQTP-COF-M (M = Zn, Ni, and Co). Adapted from ref. 107. © 2019 Elsevier B.V. All rights reserved.

CH_3OH (74%) and CH_3CH_2OH (26%) with a total yield of 798 mol g^{-1}. The synergy in both the bimetallic NCs and the cluster@N3-COF assisted significantly in the interfacial charge transfer and C–C coupling, resulting in good photoactivity for CO_2 reduction to C_1/C_2 alcohols. In order to better understand the C–C coupling, *in situ* FTIR studies were performed during the photoreduction of CO_2 and a possible reaction mechanism was also predicted by predicting the surface molecules produced during photocatalysis.

You *et al.* demonstrated a heterogeneous photocatalytic system based on an iridium complex (Ir-ppy) and hydrazone-based COF (NAHN-Tp), which acts as a photosensitizer and can absorb visible light energy.[128] The formed 2D hydrazone-based COF synthesized from 1,3,5-triformylphloroglucinol (Tp) and *N*-amino-4-hydrazino-1,8-naphthalimide (NAHN) and combined with NAHN-Tp(Ir-ppy) took part in the photochemical CO_2 reduction to CO [Fig. 8].

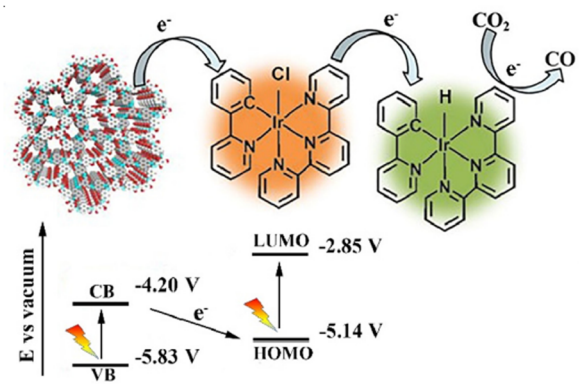

Fig. 8 Z-scheme electron transfer during CO_2 reduction using a NAHN-Tp and [Ir-ppy]. Adapted from ref. 128. © 2020 Published by Elsevier Inc.

2.1.3. Photo-electrocatalytic CO_2 reduction (PCER). For the first time, Lan's group published dioxin-linked metallophthalocyanine covalent organic frameworks as photo-coupled CO_2 reduction electrocatalysts in 2020.[126] In this study, they designed a series of crystalline and stable dioxin-linked metallophthalocyanine covalent organic frameworks (MPc-TFPN COF, M = Ni, Co, Zn), among which NiPc/CoPc-TFPN COF showed excellent activity for CO_2 reduction when coupled with light compared to a dark environment. The reaction mechanism was also studied by DFT, which revealed that an external light field can improve the electron transfer to the adsorbed CO_2 in phthalocyanine COFs leading to the favorable CO_2. DFT calculation results indicated that in the COF systems, the N atom in the phthalocyanine ligand plays a major role in adsorbing and activating CO_2. The free energy change for CO_2 adsorption on the central metal in

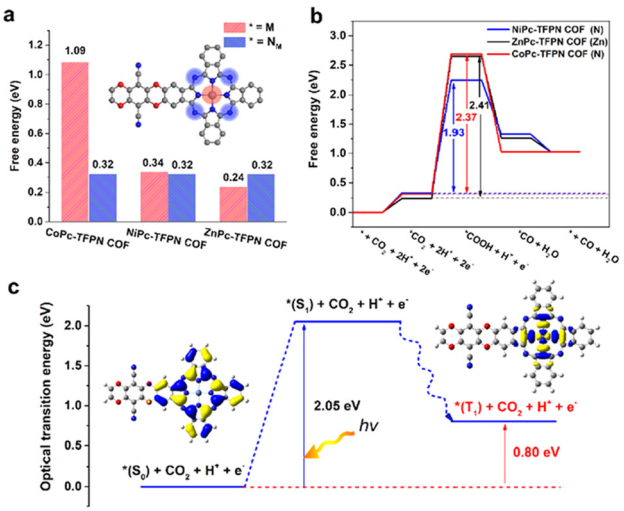

Fig. 9 (a) Mechanism and DFT calculations. (a) A comparison of the relative adsorption energy for the first step of ECR (* + CO_2 + $2H^+$ + $2e^-$ → *CO_2 + $2H^+$ + $2e^-$) on the metal site (red) and nitrogen site (blue) on MPc-TFPN COF, (b) the free energy diagrams for CO_2 reduction to CO on MPc-TFPN COF (Note that the symbols in brackets represent the reaction sites). The rate-determining step and the corresponding free energy on each COFs are indicated, (c) schematic representation of the excited states of NiPc-TFPN COF. Adapted from ref. 126. © 2020 Wiley-VCH GmbH.

the NiPc-TFPN COF and CoPc-TFPN COF is substantially higher than the N site (NM, which means N in MPc, which is highlighted with blue background in Fig. 9a). Hence, according to the minimum energy principle, CO_2 molecules have a tendency to be adsorbed as well as activated on NM atoms in the first step of ECR *i.e.* ($* + CO_2 + 2H^+ + 2e^- \rightarrow *CO_2 + 2H^+ + 2e^-$) on these two catalysts. To understand the effect of light on the ECR, the electronic properties of S_1 and T_1 excited states for the COF catalysts were examined. The NiPc-TFPN COF was first excited from S_0 to S_1 state upon light irradiation, followed by transforming to T1 state through intersystem crossing (Fig. 9c). The energy gap between S0 and S1 was found to be 2.05 eV, and the optical transition energy of the T1 state was discovered to be 0.80 eV (*vs.* ground state), showing that the phthalocyanine COF catalysts will be driven to a higher energy-excited state under light irradiation. The free energy change is reduced from the T_1 excited state to the active centre compared to the ground state, which leads to the beneficial activation of CO_2 to *COOH. This is how they explained the inherent reason why NiPc-TFPN COF showed better PECR activity than ECR. Some of the studies on photo-electrochemical reduction of CO_2 are shown in Table 2.

A while back, Jing's group first demonstrated Cu@porphyrin-COFs nanorods by a solvothermal technique, which served as an effective photoelectrocatalyst for producing C_1–C_3 products such as CH_3OH, CH_3CH_2OH, $CH_3CH(OH)_2$ and CH_3COCH_3 with apparent faradaic efficiency (AFE) of 452.75% by CO_2 reduction.[127] The incorporation of Cu by electrodeposition on the surface of porphyrin-COFs is believed to considerably boost the rate of charge transfer by protons harvesting and outstanding absorption of light, thus favoring the C–C coupling process. Besides this, the presence of organic linkers bearing –OH groups would increase the stability of COFs by benefiting the development of intermolecular hydrogen bonds that enhance the reaction activity of CO_2 reduction. However, some of the studies on photo-electrochemical CO_2 reduction are shown in Table 2, which suggests that these findings pave the path for designing innovative and highly active photoelectrocatalysts for effective PEC CO_2 reduction. PCER can explore a new strategy toward the reduction of CO_2 in the near future as there are hardly any reported experiments explored in this field yet.

3. Shortcomings of COFs

The synthesis of a broad range of COFs mainly depends on the involved reversible reactions, which generate a significant drawback associated with the chemical stability of the COFs. During this reversible COF formation process, water is produced as a by-product, which boosts the reaction in the backward direction. As a result, the decomposition of COFs occurs, which restricts the employment of COFs in rational industrial applications along with other spacious utilizations such as gas storage, sensors, and catalysis. Hence, the development of COFs having greater stability in aqueous and organic conditions serves as a driving factor in this field of research. In order to develop stable COFs, many academic disciplines give huge efforts to rational design and synthesis of COFs, which can maintain their porosity and crystallinity under harsh environmental conditions.[134] For the production of stable COFs, two methods have been established until now, firstly, using stable organic linkers and the second one is to form intramolecular and interlayer hydrogen bonds.[135]

One of the main disadvantages of COFs for electrochemical applications is their poor electrical conductivity even though COFs exhibit a large surface area. Considering the existence of active sites present in the COF framework, a specific charge-transport route is required for effective electrocatalytic activities. By using the right building blocks and synthetic methods or by the assimilation of extremely conductive units (such as thiophene and thieno-thiophene derivatives) into the COF framework, this intrinsic drawback can be overcome.[136]

4. Future scope and conclusions

In conclusion, covalent organic frameworks (COFs) are particularly promising CO_2 reduction catalysts for next-generation applications. They have multiple advantages over traditional heterogeneous catalysts such as metal-oxide, noble-metal plasmonic inorganic semiconductors, and inorganic–organic hybrid MOF-based catalysts. COFs are composed of organic moieties and non-metal elements; therefore, the COF's monomer units are low-cost and more readily available than metal-containing inorganic catalysts and MOFs. The electronic and steric factors in COF can be tuned conveniently using different monomer units, which allow us to modify the structure of COF, which are more suitable for CO_2 adsorption and reduction reactions. As shown in Table 2, most of the reported literature dedicated to COF-based catalytic CO_2RR is focused on the development of hybrid materials, which combine semiconductor COF with various metals or other conductive materials. In this way, fine-tuning the various parameters involved in the construction of a heterogeneous nanohybrid, for instance, heterojunction formed between both molecular units, their corresponding molar ratios, or the precise site of the dopant on the catalyst, could have an impact on both the electronic structure of the COF and its active sites, and thus, are the important factors in determining the catalytic properties. Comparatively, low reaction yields that presently impede more advancements in this arena can be improved through the logical regulation of such factors. Even though COFs as CO_2 reduction catalysts have multiple advantages, there are still many spaces to address some challenges, which need to be resolved in this area of research. Primarily, the use of the SARS in the photocatalytic CO_2 reduction reaction is severely constrained by the ambiguity of the COF structure. Secondly, the significant difficulty in generating a great sufficient 2D COF single-crystal for typical X-ray single-crystal diffraction characterization continues to limit the construction of 2D COFs for a variety of applications, including catalytic CO_2 reduction. In spite of the fact that photo-coupled electrochemical reduction is a promising method for CO_2 reduction, the PCER method is poorly explored using COFs as heterogeneous catalysts. On the other hand, the

major issue is the reaction mechanism, which must be decoded soon so that we could design more effective COFs for CO_2 reduction. Therefore, if the above-addressed issues are properly addressed COFs-based materials can contribute immensely as CO_2 reduction catalysts to achieve sustainable energy and environment in the future.

Conflicts of interest

There are no conflicts to declare.

Acknowledgements

SMI acknowledges the Department of Science and Technology DST-SERB (project reference no. CRG/2020/000244), New Delhi, Govt. of India and Council of Scientific and Industrial and Research, CSIR (project reference no. 02(0453)/21/EMR-II dated 08/06/2021), New Delhi, Govt. of India and Board of Research in Nuclear Sciences (BRNS), Govt. of India, (project reference no. 58/14/15/2022-BRNS/37077) for providing financial support. PS is thankful to CSIR, India (09/106(0178)/2018-EMR-I) for her fellowship. I. H. C. is thankful to CSIR, India (09/106(0181)/2019-EMR-I) for her fellowship. SD is thankful to SVMCM, Govt. of West Bengal for her fellowship. We acknowledge the DST for providing a grant to the Department of Chemistry by FIST and PURSE grant.

Notes and references

1 (*a*) W.-H. Wang, Y. Himeda, J. T. Muckerman, G. F. Manbeck and E. Fujita, *Chem. Rev.*, 2015, **115**, 12936–12973; (*b*) J. C. Zachos, G. R. Dickens and R. E. Zeebe, *Nature*, 2008, **451**, 279–283.

2 Y. Izumi, *Coord. Chem. Rev.*, 2013, **257**, 171–186.

3 A. Gore, *An Inconvenient Truth*, The Wylie Agency, London, UK, 2006, p. 66.

4 (*a*) A. Kubacka, M. Fernández-García and G. Colón, *Chem. Rev.*, 2012, **112**, 1555–1614; (*b*) S. Wang and X. Wang, *Appl. Catal., B*, 2015, **162**, 494–500; (*c*) I. H. Chowdhury, A. H. Chowdhury, P. Sarkar and S. M. Islam, *ChemNanoMat*, 2021, **7**, 580–591; (*d*) A. H. Chowdhury, I. H. Chowdhury, S. Biswas and S. M. Islam, *Mol. Catal.*, 2020, **493**, 111050; (*e*) A. H. Chowdhury, I. H. Chowdhury and S. M. Islam, *Ind. Eng. Chem. Res.*, 2019, **58**, 11779–11786; (*f*) A. H. Chowdhury, A. Das, S. Riyajuddin, K. Ghosh and S. M. Islam, *Catal. Sci. Tech.*, 2019, **9**, 6566–6569; (*g*) I. H. Chowdhury, A. H. Chowdhury, P. Sarkar and S. M. Islam, *ChemNanoMat*, 2021, **7**, 580–591; (*h*) A. H. Chowdhury, I. H. Chowdhury, S. Biswas and S. M. Islam, *Mol. Catal.*, 2020, **493**, 111050; (*i*) A. H. Chowdhury, I. H. Chowdhury and S. M. Islam, *Ind. Eng. Chem. Res.*, 2019, **58**, 11779–11786; (*j*) S. Ghosh, R. A. Molla, U. Kayal, A. Bhaumik and S. M. Islam, *Dalton Trans.*, 2019, **48**, 4657–4666; (*k*) S. M. Islam, A. S. Roy, P. Mondal and N. Salam, *J. Mol. Catal. A: Chem.*, 2012, **358**, 38–48; (*l*) N. Haque, S. Biswas, P. Basu, I. H. Biswas, R. Khatun, A. Khan and S. M. Islam, *New J. Chem.*, 2020, **44**, 15446–15458; (*m*) A. Sahoo, A. H. Chowdhury, P. Singha, A. Banerjee, S. M. Islam and T. Bala, *Mol. Catal.*, 2020, **493**, 111070; (*n*) P. Bhanja, K. Ghosh, S. S. Islam, A. K. Patra, S. M. Islam and A. Bhaumik, *ACS Sustainable Chem. Eng.*, 2016, **4**(12), 7147–7157; (*o*) S. Roy, P. Bhanja, S. S. Islam, A. Bhaumik and S. M. Islam, *Chem. Commun.*, 2016, **52**, 1871; (*p*) S. Roy, B. Banerjee, A. Bhaumik and S. M. Islam, *RSC Adv.*, 2016, **6**, 31153–31160; (*q*) S. Bhunia, R. A. Molla, V. Kumari, S. M. Islam and A. Bhaumik, *Chem. Commun.*, 2015, **51**, 15732; (*r*) S. Roy, T. Chatterjee, B. Banerjee, N. Salam, A. Bhaumik and S. M. Islam, *RSC Adv*, 2014, **4**(86), 46075–46083; (*s*) R. A. Molla, K. Ghosh, K. Tuhina and S. M. Islam, *New J. Chem.*, 2015, **39**(2), 921–930; (*t*) S. M. Islam, A. S. Roy, P. Mondal, S. Paul and N. Salam, *Inorg. Chem. Commun.*, 2012, **24**, 170–176; (*u*) S. M. Islam, D. Mal, B. K. Palit and C. R. Saha, *J. Mol. Catal. A: Chem.*, 1999, **142**(2), 169–181; (*v*) S. M. Islam, N. Salam, P. Mondal, A. S. Roy, K. Ghosh and K. Tuhina, *J. Mol. Catal. A: Chem.*, 2014, **387**, 7–19; (*w*) S. Roy, B. Banerjee, N. Salam, A. Bhaumik and S. M. Islam, *ChemCatChem*, 2015, **7**(17), 2689–2697; (*x*) S. M. Islam, R. A. Molla, A. S. Roy and K. Ghosh, *RSC Adv.*, 2014, **4**(50), 26181–26192; (*y*) S. M. Islam, R. A. Molla, A. S. Roy and K. Ghosh, *RSC Adv.*, 2014, **4**(50), 26181–26192; (*z*) A. H. Chowdhury, S. Ghosh and S. M. Islam, *New J. Chem.*, 2018, **42**(17), 14194–14202.

5 (*a*) G. Centi, E. A. Quadrelli and S. Perathoner, *Energy Environ. Sci.*, 2013, **6**, 1711–1731; (*b*) W. Wang, S. Wang, X. Ma and J. Gong, *Chem. Soc. Rev.*, 2011, **40**, 3703–3727; (*c*) P. Sarkar, A. H. Chowdhury, S. Riyajuddin, S. Biswas, K. Ghosh and S. M. Islam, *New J. Chem.*, 2020, **44**, 744–752; (*d*) P. Chakrabortty, A. Das, A. H. Chowdhury, S. Ghosh, A. Khan and S. M. Islam, *New J. Chem.*, 2021, **45**, 4738–4745; (*e*) P. Sarkar, A. H. Chowdhury, S. Biswas, A. Khan and S. M. Islam, *Mater. Today Chem.*, 2021, **21**, 100509; (*f*) S. Das, I. H. Chowdhury, A. Chakraborty, M. K. Naskar, M. Sarkar and S. M. Islam, *Mater. Adv.*, 2022, **3**, 3165–3173; (*g*) R. Khatun, S. Biswas, S. Islam, I. H. Biswas, S. Riyajuddin, K. Ghosh and S. M. Islam, *ChemCatChem*, 2019, **11**(4), 1303–1312; (*h*) A. H. Chowdhury, S. Ghosh and S. M. Islam, *New J. Chem.*, 2018, **42**(17), 14194–14202; (*i*) R. Khatun, P. Bhanja, P. Mondal, A. Bhaumik, D. Das and S. M. Islam, *New J. Chem.*, 2017, **41**(21), 12937–12946; (*j*) R. A. Molla, M. A. Iqubal, K. Ghosh and S. M. Islam, *Green Chem.*, 2016, **18**(17), 4649–4656; (*k*) R. Khatun, S. Biswas, I. H. Biswas, S. Riyajuddin, N. Haque and K. Ghosh, *J. CO2 Util.*, 2020, **40**, 101180; (*l*) P. Sarkar, S. Riyajuddin, A. Das, A. H. Chowdhury, K. Ghosh and S. M. Islam, *Mol. Catal.*, 2020, **484**, 110730; (*m*) S. Sarkar, S. Ghosh and S. M. Islam, *Org. Biomol. Chem.*, 2022, **20**(8), 1707–1722; (*n*) U. Mandi, A. S. Roy, S. K. Kundu, S. Roy, A. Bhaumik and S. M. Islam, *J. Colloid Interface Sci.*, 2016, **472**, 202–209; (*o*) R. A. Molla, A. S. Roy, K. Ghosh, N. Salam, M. A. Iqubal,

K. Tuhina and S. M. Islam, *J. Organomet. Chem.*, 2014, **776**, 170–179; (*p*) U. Mandi, A. S. Roy, B. Banerjee and S. M. Islam, *RSC Adv.*, 2014, **4**(80), 42670–42681; (*q*) R. Khatun, P. Bhanja, R. A. Molla, S. Ghosh, A. Bhaumik and S. M. Islam, *Mol. Catal.*, 2017, **434**, 25–31; (*r*) I. H. Biswas, S. Biswas, M. S. Islam, S. Riyajuddin, P. Sarkar and K. Ghosh, *New J. Chem.*, 2019, **43**(36), 14643–14652; (*s*) T. K. Dey, K. Ghosh, P. Basu, R. A. Molla and S. M. Islam, *New J. Chem.*, 2018, **42**(11), 9168–9176; (*t*) N. Salam, P. Paul, S. Ghosh, U. Mandi, A. Khan, S. M. Alam, D. Das and S. M. Islam, *New J. Chem.*, 2020, **44**(14), 5448–5456; (*u*) R. K. Mondal, S. Riyajuddin, A. Ghosh, S. Ghosh, K. Ghosh and S. M. Islam, *J. Organomet. Chem.*, 2019, **880**, 322–332; (*v*) S. Das, P. Mondal, S. Ghosh, B. Satpati, S. Deka, S. M. Islam and T. Bala, *New J. Chem.*, 2018, **42**(9), 7314–7325; (*w*) S. Sarkar, S. Ghosh, J. Mondal and S. M. Islam, *Chem. Commun.*, 2020, **56**(81), 12202–12205; (*x*) N. Haque, S. Biswas, P. Basu, I. H. Biswas, R. Khatun, A. Khan and S. M. Islam, *New J. Chem.*, 2020, **44**(36), 15446–15458; (*y*) I. H. Chowdhury, A. H. Chowdhury, A. Das, A. Khan and S. M. Islam, *New J. Chem.*, 2020, **44**(27), 11720–11726; (*z*) M. Islam, A. S. Roy and S. Islam, *Catal. Lett.*, 2016, **146**(6), 1128–1138.

6 (*a*) J. Mao, T. Peng, X. Zhang, K. Li and L. Zan, *Catal. Commun.*, 2012, **28**, 38–41; (*b*) M. Tahir and N. S. Amin, *Energy Convers. Manag.*, 2013, **76**, 194–214; (*c*) H. Yang, J. Yan, Z. Lu, X. Cheng and Y. Tang, *J. Alloys Compd.*, 2009, **476**, 715–719.

7 (*a*) P. De Luna, R. Quintero-Bermudez, C.-T. Dinh, M. B. Ross, O. S. Bushuyev, P. Todorović, T. Regier, S. O. Kelley, P. Yang and E. H. Sargent, *Nat. Catal.*, 2018, **1**, 103–110; (*b*) P. De Luna, C. Hahn, D. Higgins, S. A. Jaffer, T. F. Jaramillo and E. H. Sargent, *Science*, 2019, **364**, eaav 3506; (*c*) V. S. Thoi, N. Kornienko, C. G. Margarit, P. D. Yang and C. J. Chang, *J. Am. Chem. Soc.*, 2013, **135**, 14413–14424; (*d*) E. E. Barton, D. M. Rampulla and A. B. Bocarsly, *J. Am. Chem. Soc.*, 2008, **130**, 6342–6344.

8 T. Inoue, A. Fujishima, S. Konishi and K. Honda, *Nature*, 1979, **277**, 637–638.

9 (*a*) S. Yang, W. Hu, X. Zhang, P. He, B. Pattengale, C. Liu, M. Cendejas, I. Hermans, X. Zhang, J. Zhang and J. Huang, *J. Am. Chem. Soc.*, 2018, **140**, 14614–14618; (*b*) P. Sarkar, S. Riyajuddin, A. Das, A. H. Chowdhury, K. Ghosh and S. M. Islam, *Mol. Catal.*, 2020, **484**, 110730; (*c*) N. Huang, P. Wang and D. Jiang, *Nat. Rev. Mater.*, 2016, **1**, 1–19; (*d*) M. S. Lohse and T. Bein, *Adv. Funct. Mater.*, 2018, **28**, 1705553; (*e*) C. S. Diercks and O. M. Yaghi, *Science*, 2017, **355**, eaal1585; (*f*) S. L. Cai, W. G. Zhang, R. N. Zuckermann, Z. T. Li, X. Zhao and Y. Liu, *Adv. Mater.*, 2015, **27**, 5762–5770; (*g*) Y. Song, Q. Sun, B. Aguila and S. Ma, *Adv. Sci.*, 2019, **6**, 1801410; (*h*) I. Omae, *Coord. Chem. Rev.*, 2012, **256**, 1384–1405; (*i*) S. Ghosh, S. Riyajuddin, S. Sarkar, K. Ghosh and S. M. Islam, *ChemNanoMat*, 2020, **6**, 160–172; (*j*) S. Ghosh, P. Mondal, D. Das, K. Tuhina and S. M. Islam, *J. Organomet. Chem.*, 2018, **866**, 1–12; (*k*) N. Salam, P. Paul, S. Ghosh, U. Mandi, A. Khan, S. M. Alam, D. Das and S. M. Islam, *New J. Chem.*, 2020, **44**, 5448–5456; (*l*) S. S. Islam, N. Salam, R. A. Molla, S. Riyajuddin, N. Yasmin, D. Das and K. Ghosh, *Mol. Catal.*, 2019, **477**, 110541; (*m*) R. K. Mondal, S. Riyajuddin, A. Ghosh, S. Ghosh, K. Ghosh and S. M. Islam, *J. Organomet. Chem.*, 2019, **880**, 322–332; (*n*) S. Biswas, D. Roy, S. Ghosh and S. M. Islam, *J. Organomet. Chem.*, 2019, **898**, 120877; (*o*) A. Das, R. K. Mondal, P. Chakrabortty, S. Riyajuddin and A. H. Chowdhury, *Mol. Catal.*, 2021, **499**, 111253; (*p*) S. M. Islam, A. S. Roy, P. Mondal, S. Paul and N. Salam, *Inorg. Chem. Commun.*, 2012, **24**, 170–1762012; (*q*) S. M. Islam, D. Mal, B. K. Palit and C. R. Saha, *J. Mol. Catal. A: Chem.*, 1999, **142**(2), 169–181; (*r*) R. A. Molla, K. Ghosh, K. Tuhina and S. M. Islam, *New J. Chem.*, 2015, **39**(2), 921–930; (*s*) S. Ghosh, P. Bhanja, N. Salam, R. Khatun, A. Bhaumik and S. M. Islam, *Catal. Today*, 2018, **309**, 253–262; (*t*) R. Khatun, P. Bhanja, R. A. Molla, S. Ghosh, A. Bhaumik and S. M. Islam, *Mol. Catal.*, 2017, **434**, 25–31; (*u*) I. H. Biswas, S. Biswas, M. S. Islam, S. Riyajuddin, P. Sarkar and K. Ghosh, *New J. Chem.*, 2019, **43**(36), 14643–14652; (*v*) S. Biswas, R. Khatun, M. Dolai, I. H. Biswas, N. Haque, M. Sengupta and M. S. Islam, *New J. Chem.*, 2020, **44**(1), 141–151; (*w*) S. Biswas, D. Roy, S. Ghosh and S. M. Islam, *J. Organomet. Chem.*, 2019, **898**, 120877; (*x*) S. Ghosh, A. Ghosh, S. Riyajuddin, S. Sarkar, A. H. Chowdhury and K. Ghosh, *ChemCatChem*, 2020, **12**(4), 1055–1067; (*y*) S. Ghosh, S. Riyajuddin, S. Sarkar, K. Ghosh and S. M. Islam, *ChemNanoMat*, 2020, **6**(1), 160–172; (*z*) S. M. Islam, A. S. Roy, P. Mondal, S. Paul and N. Salam, *Inorg. Chem. Commun.*, 2012, **24**, 170–176.

10 (*a*) H. M. El-Kaderi, J. R. Hunt, J. L. Mendoza-Cortes, A. P. Cote, R. E. Taylor, M. O'Keeffe and O. M. Yaghi, *Science*, 2007, **316**, 268–272; (*b*) R. A. Molla, M. A. Iqubal, K. Ghosh and S. M. Islam, *Green Chem.*, 2016, **18**, 4649–4656; (*c*) R. Khatun, S. Biswas, I. H. Biswas, S. Riyajuddin, N. Haque and K. Ghosh, *J. CO2 Util.*, 2020, **40**, 101180; (*d*) R. Khatun, P. Bhanja, R. A. Molla, S. Ghosh, A. Bhaumik and S. M. Islam, *Mol. Catal.*, 2017, **434**, 25–31; (*e*) S. Biswas, R. Khatun, M. Dolai, I. H. Biswas, N. Haque, M. Sengupta and S. M. Islam, *New J. Chem.*, 2020, **44**, 141–151; (*f*) I. H. Biswas, S. Biswas, M. S. Islam, S. Riyajuddin, P. Sarkar and K. Ghosh, *New J. Chem.*, 2019, **43**, 14643–14652; (*g*) S. Ghosh, A. Ghosh, S. Riyajuddin, S. Sarkar, A. H. Chowdhury and K. Ghosh, *ChemCatChem*, 2020, **12**, 1055–1067; (*h*) S. Sarkar, S. Ghosh, J. Mondal and S. M. Islam, *Chem. Commun.*, 2020, **56**, 12202–12205; (*i*) T. K. Dey, P. Bhanja, P. Basu, A. Ghosh and S. M. Islam, *ChemistrySelect*, 2019, **4**, 14315–14328; (*j*) S. Ghosh, A. Ghosh, S. Biswas, M. Sengupta, D. Roy and S. M. Islam, *ChemistrySelect*, 2019, **4**, 3961–3972; (*k*) S. S. Islam, S. Biswas, R. Ali Molla, N. Yasmin and S. M. Islam, *ChemNanoMat*, 2020, **6**, 1386–1397; (*l*) P. Basu, T. K. Dey, S. Riyajuddin,

S. Biswas, K. Ghosh and S. M. Islam, *New J. Chem.*, 2020, **44**, 12680–126919; (*m*) R. Khatun, S. Biswas, S. Islam, I. H. Biswas, S. Riyajuddin, K. Ghosh and S. M. Islam, *ChemCatChem*, 2019, **11**, 1303–1312; (*n*) M. Sengupta, A. Bag, S. Ghosh, P. Mondal, A. Bordoloi and S. M. Islam, *J. CO2 Util.*, 2019, **34**, 533–542; (*o*) A. H. Chowdhury, S. Ghosh and S. M. Islam, *New J. Chem.*, 2018, **42**, 14194–14202; (*p*) R. Khatun, P. Bhanja, P. Mondal, A. Bhaumik, D. Das and S. M. Islam, *New J. Chem.*, 2017, **41**, 12937–12946; (*q*) A. H. Chowdhury, U. Kayal, I. H. Chowdhury, S. Ghosh and S. M. Islam, *ChemistrySelect*, 2019, **4**, 1069–1077; (*r*) S. Ghosh, P. Bhanja, N. Salam, R. Khatun, A. Bhaumik and S. M. Islam, *Catal. Today*, 2018, **309**, 253–262; (*s*) R. A. Molla, K. Ghosh, K. Tuhina and S. M. Islam, *New J. Chem.*, 2015, **39**(2), 921–930; (*t*) M. Islam, A. S. Roy and S. Islam, *Cat. Lett.*, 2016, **146**(6), 1128–1138; (*u*) S. M. Islam, N. Salam, P. Mondal, A. S. Roy, K. Ghosh and K. Tuhina, *J. Mol. Catal. A: Chem.*, 2014, **387**, 7–19; (*v*) S. Roy, B. Banerjee, N. Salam, A. Bhaumik and S. M. Islam, *ChemCatChem*, 2015, **7**(17), 2689–2697; (*w*) S. M. Islam, R. A. Molla, A. S. Roy and K. Ghosh, *RSC Adv.*, 2014, **4**(50), 26181–26192; (*x*) S. Roy, T. Chatterjee, B. Banerjee, N. Salam, A. Bhaumik and S. M. Islam, *RSC Adv.*, 2014, **4**(86), 46075–46083; (*y*) S. Ghosh, T. S. Khan, A. Ghosh, A. H. Chowdhury, M. A. Haider and A. Khan, *ACS Sustainable Chem. Eng.*, 2020, **8**(14), 5495–5513; (*z*) R. Khatun, P. Bhanja, P. Mondal, A. Bhaumik, D. Das and S. M. Islam, *New J. Chem.*, 2017, **41**(21), 12937–12946.

11 A. P. Cote, A. I. Benin, N. W. Ockwig, M. O'Keeffe, A. J. Matzger and O. M. Yaghi, *Science*, 2005, **310**, 1166–1170.

12 N. L. Campbell, R. Clowes, L. K. Ritchie and A. I. Cooper, *Chem. Mater.*, 2009, **21**, 204–206.

13 B. P. Biswal, S. Chandra, S. Kandambeth, B. Lukose, T. Heine and R. Banerjee, *J. Am. Chem. Soc.*, 2013, **135**, 5328–5331.

14 D. D. Medina, J. M. Rotter, Y. Hu, M. Dogru, V. Werner, F. Auras, J. T. Markiewicz, P. Knochel and T. Bein, *J. Am. Chem. Soc.*, 2015, **137**, 1016–1019.

15 S. B. Kalidindi, H. Oh, M. Hirscher, D. Esken, C. Wiktor, S. Turner, G. Van Tendeloo and R. A. Fischer, *Chem. – Eur. J.*, 2012, **18**, 10848–10856.

16 T. Ben and S. Qiu, *CrstEngComm*, 2013, **15**, 17–26.

17 S. Y. Ding and W. Wang, *Chem. Soc. Rev.*, 2013, **42**, 548–568.

18 Q. Fang, Z. Zhuang, S. Gu, R. B. Kaspar, J. Zheng, J. Wang, S. Qiu and Y. Yan, *Nat. Commun.*, 2014, **5**, 1–8.

19 (*a*) M. Wu, G. Chen, P. Liu, W. Zhou and Q. Jia, *Analyst*, 2016, **141**, 243–250; (*b*) A. Das, R. K. Mondal, P. Chakrabortty, S. Riyajuddin, A. H. Chowdhury, S. Ghosh, A. Khan, K. Ghosh and S. M. Islam, *Mol. Catal.*, 2021, **499**, 111253; (*c*) M. Sengupta, A. Bag, S. Ghosh, P. Mondal, A. Bordoloi and S. M. Islam, *J. CO2 Util.*, 2019, **34**, 533–542; (*d*) S. S. Islam, S. Biswas, R. A. Molla, N. Yasmin and S. M. Islam, *ChemNanoMat*, 2020, **6**, 1386–1397; (*e*) M. Islam, A. S. Roy and S. Islam, *Catal. Lett.*, 2016, **146**(6), 1128–1138; (*f*) N. Haque, S. Biswas, S. Ghosh, A. H. Chowdhury, A. Khan and S. M. Islam, *ACS Appl. Nano Mater.*, 2021, **4**, 7663–7674; (*g*) S. Sarkar, S. Ghosh, J. Mondal and S. M. Islam, *Chem. Commun.*, 2020, **56**, 12202–12205; (*h*) S. Sarkar, S. Ghosh and S. M. Islam, *Org. Biomol. Chem.*, 2022, **20**, 1707–1722; (*i*) P. Sarkar, A. H. Chowdhury, S. Riyajuddin, S. Biswas, K. Ghosh and S. M. Islam, *New J. Chem.*, 2020, **44**, 744–752; (*j*) P. Chakrabortty, A. Das, A. H. Chowdhury, S. Ghosh, A. Khan and S. M. Islam, *New J. Chem.*, 2021, **45**, 4738–4745; (*k*) P. Sarkar, A. H. Chowdhury, S. Biswas, A. Khan and S. M. Islam, *Mater. Today Chem.*, 2021, **21**, 100509; (*l*) S. Biswas, R. Khatun, M. Sengupta and S. M. Islam, *Mol. Catal.*, 2018, **452**, 129–137; (*m*) S. Roy, B. Banerjee, A. Bhaumik and S. M. Islam, *RSC Adv.*, 2016, **6**, 31153–31160; (*n*) S. Ghosh, P. Bhanja, R. A. Molla, R. Khatun and S. M. Islam, *ChemistrySelect*, 2017, **2**, 2159–2165; (*o*) I. H. Chowdhury, A. H. Chowdhury, A. Das, A. Khan and S. M. Islam, *New J. Chem.*, 2020, **44**, 11720–11726; (*p*) P. Sarkar, S. Riyajuddin, A. Das, A. H. Chowdhury, K. Ghosh and S. M. Islam, *Mol. Catal.*, 2020, **484**, 110730; (*q*) S. M. Islam, N. Salam, P. Mondal and A. S. Roy, *J. Mol. Catal. A: Chem.*, 2013, **366**, 321–332; (*r*) S. M. Islam, P. Mondal, S. Mukherjee, A. S. Roy and A. Bhaumik, *Polym. Adv. Technol.*, 2011, **22**(6), 933–941; (*s*) M. Sengupta, A. Bag, S. Ghosh, P. Mondal, A. Bordoloi and S. M. Islam, *J. CO2 Util.*, 2019, **34**, 533–542; (*t*) A. H. Chowdhury, S. Ghosh and S. M. Islam, *New J. Chem.*, 2018, **42**(17), 14194–14202; (*u*) S. M. Islam, P. Mondal, S. Mukherjee, A. S. Roy and A. Bhaumik, *Polym. Adv. Technol.*, 2011, **22**(6), 933–941; (*v*) S. M. Islam, A. Bose, B. K. Palit and C. R. Saha, *J. Catal.*, 1998, **173**(2), 268–281; (*w*) S. Roy, T. Chatterjee, B. Banerjee, N. Salam, A. Bhaumik and S. M. Islam, *RSC Adv.*, 2014, **4**(86), 46075–46083; (*x*) S. K. Das, B. K. Chandra, R. A. Molla, M. Sengupta, S. M. Islam and A. Majee, *Mol. Catal.*, 2020, **480**, 110650; (*y*) P. Basu, P. Bhanja, N. Salam, T. K. Dey, A. Bhaumik, D. Das and S. M. Islam, *Mol. Catal.*, 2017, **439**, 31–40; (*z*) N. Salam, P. Mondal, J. Mondal, A. S. Roy, A. Bhaumik and S. M. Islam, *RSC Adv.*, 2012, **2**(16), 6464–6477.

20 A. Shahvar, R. Soltani, M. Saraji, M. Dinari and S. Alijani, *J. Chromatogr. A*, 2018, **1565**, 48–56.

21 T. Sick, A. G. Hufnagel, J. Kampmann, I. Kondofersky, M. Calik, J. M. Rotter, A. Evans, M. Döblinger, S. Herbert, K. Peters, D. Böhm, P. Knochel, D. D. Medina, D. Fattakhova-Rohlfing and T. Bein, *J. Am. Chem. Soc.*, 2018, **140**, 2085–2092.

22 L. Ma, S. Wang, X. Feng and B. Wang, *Chin. Chem. Lett.*, 2016, **27**, 1383–1394.

23 (*a*) V. Hasija, S. Patial, P. Raizada, A. A. P. Khan, A. M. Asiri, Q. Van Le, V. H. Nguyen and P. Singh, *Coord. Chem. Rev.*, 2022, **452**, 214298; (*b*) H. Wang, H. Wang, Z. Wang, L. Tang, G. Zeng, P. Xu, M. Chen, T. Xiong, C. Zhou, X. Liand and D. Huang, *Chem. Soc. Rev.*, 2020, **49**,

4135–4165; (*c*) D. G. Wang, T. Qiu, W. Guo, Z. Liang, H. Tabassum, D. Xiaand and R. Zou, *Energy Environ. Sci.*, 2021, **14**, 688–728; (*d*) J. You, Y. Zhao, L. Wangand and W. Bao, *J. Cleaner Prod.*, 2021, **291**, 125822.

24 (*a*) R. B. Woodward, *Pure Appl. Chem.*, 1973, **33**, 145–177; (*b*) E. J. Corey, *Chem. Soc. Rev.*, 1988, **17**, 111–133.

25 Z. Chen, K. Wang, X. Hu, P. Shi, Z. Guo and H. Zhan, *ACS Appl. Mater. Interfaces*, 2020, **13**, 1145–1151.

26 H. S. Xu, Y. Luo, X. Li, P. Z. See, Z. Chen, T. Ma, L. Liang, K. Leng, I. Abdelwahab, L. Wang, R. Li, X. Shi, Y. Zhou, X. F. Lu, X. Zhao, C. Liu, J. Sun and K. P. Loh, *Nat. Commun.*, 2020, **11**, 1434.

27 D. Zhu, X. Li, Y. Li, M. Barnes, C. P. Tseng, S. Khalil, M. M. Rahman, P. M. Ajayan and R. Verduzco, *Chem. Mater.*, 2021, **33**, 413–419.

28 Y. Xing, L. Yin, Y. Zhao, Z. Du, H. Q. Tan, X. Qin, W. Ho, T. Qiu and Y. G. Li, *Appl. Mater. Interfaces*, 2020, **12**, 51555–51562.

29 C. Wang, J. Tang, L. Li, J. Wan, Y. Ma, Y. Jin, J. Liu, H. Wangand and Q. Zhang, *Adv. Funct. Mater.*, 2022, 2204068.

30 M. J. Kory, M. Wörle, T. Weber, P. Payamyar, S. W. van de Poll, J. Dshemuchadse, N. Trapp and A. D. Schlüter, *Nat. Chem.*, 2014, **6**, 779–784.

31 P. Kissel, D. J. Murray, W. J. Wulftange, V. J. Catalano and B. T. King, *Nat. Chem.*, 2014, **6**, 774–778.

32 E. Vitaku and W. R. Dichtel, *J. Am. Chem. Soc.*, 2017, **139**, 12911–12914.

33 S. Wan, F. Gandara, A. Asano, H. Furukawa, A. Saeki, S. K. Dey, L. Liao, M. W. Ambrogo, Y. Y. Botros and X. Duan, *Chem. Mater.*, 2011, **23**, 4094–4097.

34 Z. Lei, Q. Yang, Y. Xu, S. Guo, W. Sun, H. Liu, L.-P. Lv, Y. Zhang and Y. Wang, *Nat. Commun.*, 2018, **9**, 1–13.

35 J. A. Ming, A. Liu, J. W. Zhao, P. Zhang, H. W. Huang, H. Lin, Z. T. Xu, X. M. Zhang, X. X. Wang, J. Hofkens, M. B. J. Roeffaers and J. L. Long, *Angew. Chem., Int. Ed.*, 2019, **58**, 18290–18294.

36 D. G. Wang, T. Qiu, W. Guo, Z. Liang, H. Tabassum, D. Xia and R. Zou, *Energy Environ. Sci.*, 2021, **14**, 688–728.

37 C. Liu, Y. Xiao, Q. Yang, Y. Wang, R. Lu, Y. Chen, C. Wang and H. Yan, *Appl. Surf. Sci.*, 2021, **537**, 148082.

38 M. Martínez-Abadía, K. Strutyński, C. T. Stoppiello, B. L. Berlanga, C. Martí-Gastaldo, A. N. Khlobystov, A. Saeki, M. Melle-Franco and A. Mateo-Alonso, *Nanoscale*, 2021, **13**, 6829–6833.

39 Y. Wang, W. Hao, H. Liu, R. Chen, Q. Pan, Z. Liand and Y. Zhao, *Nat. Commun.*, 2022, **13**, 1–7.

40 Y. Chen, Z.-L. Shi, L. Wei, B. Zhou, J. Tan, H.-L. Zhou and Y.-B. Zhang, *J. Am. Chem. Soc.*, 2019, **141**, 3298–3303.

41 H. Ding, J. Li, G. Xie, G. Lin, R. Chen, Z. Peng, C. Yang, B. Wang, J. Sun and C. Wang, *Nat. Commun.*, 2018, **9**, 1–7.

42 M. Zhang, J. Li, C. Zhang, Z. Wu, Y. Yang, J. Li, F. Fu and Z. Lin, *J. Chromatogr. A*, 2020, **1615**, 460773–460783.

43 L. Wang, Y. Chen, Z. Zhang, Y. Chen, Q. Deng and S. Wang, *Microchim. Acta*, 2021, **188**, 1–9.

44 Y. Meng, Y. Luo, J. L. Shi, H. Ding, X. Lang, W. Chen, A. Zheng, J. Sun and C. Wang, *Angew. Chem., Int. Ed.*, 2020, **59**, 3624–3629.

45 C. Gao, J. Li, S. Yin, J. Sun and C. Wang, *Nat. Commun.*, 2020, **11**, 1–8.

46 Y. Zhang, H. Li, J. Chang, X. Guan, L. Tang, Q. Fang, V. Valtchev, Y. Yan and S. Qiu, *Small*, 2021, **17**, 2006112.

47 X. Liu, J. Li, B. Gui, G. Lin, Q. Fu, S. Yin, X. Liu, J. Sun and C. Wang, *J. Am. Chem. Soc.*, 2021, **143**, 2123–2129.

48 X. Wang, M. Bahri, Z. Fu, M. A. Little, L. Liu, H. Niu, N. D. Browning, S. Y. Chong, L. Chen, J. W. Ward and A. I. Cooper, *J. Am. Chem. Soc.*, 2021, **143**, 15011–15016.

49 M. Wu, H. Huang, B. Xu and G. Zhang, *RSC Adv.*, 2022, **12**, 16354–16357.

50 Y. Du, H. Yang, J. M. Whiteley, S. Wan, Y. Jin, S. H. Lee and W. Zhang, *Angew. Chem.*, 2016, **128**, 1769–1773.

51 Y. Song, Q. Sun, B. Aguila and S. Ma, *Adv. Sci.*, 2018, **5**, 1801410.

52 S. Liu, M. Wang, T. Qian, H. Ji, J. Liu and C. Yan, *Nat. Commun.*, 2019, **10**, 3898.

53 D. Dong, H. Zhang, B. Zhou, Y. Sun, H. Zhang, M. Cao, J. Li, H. Zhou, H. Qian, Z. Lin and H. Chen, *Chem. Commun.*, 2019, **55**, 1458–1461.

54 T. Bao, S. Wang, N. Zhang and J. Zhang, *J. Chromatogr. A*, 2021, **1645**, 462130.

55 P. Puthiaraj, Y. R. Lee, S. Zhang and W. S. Ahn, *J. Mater. Chem. A*, 2016, **4**, 16288–16311.

56 J. Huo, B. Luo and Y. Chen, *ACS Omega*, 2019, **4**, 22504–22513.

57 G. Wang, T. Zhou and Y. Lei, *RSC Adv.*, 2020, **10**, 11557–11564.

58 Y. Yang, H. Niu, L. Xu, H. Zhang and Y. Cai, *Appl. Catal., B*, 2020, **269**, 118799.

59 M. Dinari and F. Jamshidian, *Polymer*, 2021, **215**, 123383.

60 C. Dai, T. He, L. Zhong, X. Liu, W. Zhen, C. Xue, S. Li, D. Jiang and B. Liu, *Adv. Mater. Interfaces*, 2021, **8**, 2002191.

61 M. Afshari, M. Dinari, K. Zargoosh and H. Moradi, *Ind. Eng. Chem. Res.*, 2020, **59**, 9116–9126.

62 M. Afshari and M. Dinari, *Composites, Part A*, 2021, **147**, 106453.

63 M. Wang, H. Guo, N. Wu, J. Zhang, T. Zhang, B. Liu, Z. Pan, L. Peng and W. Yang, *Colloids Surf., A*, 2022, **634**, 127928.

64 G. Kim, T. Shiraki and T. Fujigaya, *Bull. Chem. Soc. Jpn.*, 2020, **93**, 414–420.

65 Y. Liang, M. Xia, Y. Zhao, D. Wang, Y. Li, Z. Sui, J. Xiao and Q. Chen, *J. Colloid Interface Sci.*, 2022, **608**, 652–661.

66 M. Li, Y. Wang, S. Sun, Y. Yang, G. Gu and Z. Zhang, *Chem. Eng. J.*, 2022, **429**, 132254.

67 C. Dai, T. He, L. Zhong, X. Liu, W. Zhen, C. Xue, S. Li, D. Jiang and B. Liu, *Adv. Mater. Interfaces*, 2021, **8**, 2002191.

68 Q. Fang, J. Wang, S. Gu, R. B. Kaspar, Z. Zhuang, J. Zheng, H. Guo, S. Qiu and Y. Yan, *J. Am. Chem. Soc.*, 2015, **137**, 8352–8355.

69 Z. Wang, B. Zhang, H. Yu, L. Sun, C. Jiao and W. Liu, *Chem. Commun.*, 2010, **46**, 7730–7732.

70 J. Zhou, Y. Lei, C. Ma, W. Lv, N. Li, Y. Wang, H. Xu and Z. Zou, *Chem. Commun.*, 2017, **53**, 10536–10539.

71 R. Van Der Jagt, A. Vasileiadis, H. Veldhuizen, P. Shao, X. Feng, S. Ganapathy, N. C. Habisreutinger, M. A. Van Der

Veen, C. Wang, M. Wagemaker, S. Van Der Zwaag and A. Nagai, *Chem. Mater.*, 2021, **33**, 818–833.
72 R. Pan, J. Wu, W. Wang, C. Cheng and X. Liu, *Colloids Surf., A*, 2021, **621**, 126511.
73 N. Zhao, J. M. Liu, F. E. Yang, S. W. Lv, J. Wang and S. Wang, *ACS Appl. Bio Mater.*, 2021, **4**, 995–1002.
74 B. Sun, X. Li, T. Feng, S. Cai, T. Chen, C. Zhu, J. Zhang, D. Wang and Y. Liu, *ACS Appl. Mater. Interfaces*, 2020, **12**, 51837–51845.
75 J. Maschita, T. Banerjee, G. Savasci, F. Haase, C. Ochsenfeld and B. V. Lotsch, *Angew. Chem., Int. Ed.*, 2020, **59**, 15750–15758.
76 J. Maschita, T. Banerjee and B. V. Lotsch, *Chem. Mater.*, 2022, **34**(5), 2249–2258.
77 T. Kim, S. H. Joo, J. Gong, S. Choi, J. H. Min, Y. Kim, G. Lee, E. Lee, S. Park, S. K. Kwak and H. S. Lee, *Angew. Chem.*, 2022, **134**, 202113780.
78 F. J. Uribe-Romo, J. R. Hunt, H. Furukawa, C. Klöck, M. O. Keeffe and O. M. Yaghi, *J. Am. Chem. Soc.*, 2009, **131**, 4570–4571.
79 X. Liu, J. Li, B. Gui, G. Lin, Q. Fu, S. Yin, X. Liu, J. Sun and C. Wang, *J. Am. Chem. Soc.*, 2021, **143**, 2123–2129.
80 N. Bagherian, A. R. Karimi and A. Amini, *Colloids Surf., A*, 2021, **613**, 126078.
81 H. Wang, D. Wang, Y. Liu, Z. Wang, C. Li, S. Sun, Q. Lyu and S. Hu, *Appl. Surf. Sci.*, 2022, 152601.
82 J. Á. Martín-Illán, D. Rodríguez-San-Miguel, O. Castillo, G. Beobide, J. Perez-Carvajal, I. Imaz, D. Maspoch and F. Zamora, *Angew. Chem., Int. Ed.*, 2021, **60**, 13969–13977.
83 K. Feng, H. Hao, F. Huang, X. Lang and C. Wang, *Mater. Chem. Front.*, 2021, **5**, 2255–2260.
84 X. Wu, X. Zhang, Y. Li, B. Wang, Y. Li and L. Chen, *J. Mater. Sci.*, 2021, **56**, 2717–2724.
85 R. Bu, L. Zhang, L. L. Gao, W. J. Sun, S. L. Yang and E. Q. Gao, *J. Mol. Catal.*, 2021, **499**, 111319.
86 R. Chen, Y. Wang, Y. Ma, A. Mal, X. Y. Gao, L. Gao, L. Qiao, X. B. Li, L. Z. Wu and C. Wang, *Nat. Commun.*, 2021, **12**, 1–9.
87 N. Bagherian, A. R. Karimi and A. Amini, *Colloids Surf., A*, 2021, **613**, 126078.
88 L. R. Ahmed, A. F. EL-Mahdy, C. T. Pan and S. W. Kuo, *Adv. Mater.*, 2021, **2**, 4617–4629.
89 D. M. Li, S. Y. Zhang, J. Y. Wan, W. Q. Zhang, Y. L. Yan, X. H. Tang, S. R. Zheng, S. L. Cai and W. G. Zhang, *CrystEngComm*, 2021, **23**, 3594–3601.
90 S. Wu, Y. F. Zhang, H. Ding, X. Li and X. Lang, *J. Colloid Interface Sci.*, 2022, **610**, 446–454.
91 W. Gong, C. Liu, H. Shi, M. Yin, W. Li, Q. Song, Y. Dong and C. Zhang, *J. Mater. Chem. C*, 2022, **10**, 3553–3559.
92 P. J. Waller, S. J. Lyle, T. M. Osborn Popp, C. S. Diercks, J. A. Reimer and O. M. Yaghi, *J. Am. Chem. Soc.*, 2016, **138**, 15519–15522.
93 Z. B. Zhou, X. H. Han, Q. Y. Qi, S. X. Gan, D. L. Ma and X. Zhao, *J. Am. Chem. Soc.*, 2022, **144**, 1138.
94 H. L. Qian, F. L. Meng, C. X. Yang and X. P. Yan, *Angew. Chem., Int. Ed.*, 2020, **59**, 17607–17613.
95 S. Wu, N. Ding, P. Jiang, L. Wu, Q. Feng, L. Zhao, Y. Wang, Q. Su, H. Zhang and Q. Yang, *Tetrahedron Lett.*, 2020, **61**, 152656.
96 S. Ma, Z. Li, J. Jia, Z. Zhang, H. Xia, H. Li, X. Chen, Y. Xu and X. Liu, *Chin. J. Catal.*, 2021, **42**, 2010–2019.
97 P. Das and S. K. Mandal, *ACS Appl. Mater. Interfaces*, 2021, **13**, 14160–14168.
98 Z. Li, J. A. Wang, S. Ma, Z. Zhang, Y. Zhi, F. Zhang, H. Xia, G. Henkelman and X. Liu, *Appl. Catal., B*, 2022, **310**, 121335.
99 Z. Yang, J. Liu, Y. Li, G. Zhang, G. Xing and L. Chen, *Angew. Chem., Int. Ed.*, 2021, **60**, 20754–20759.
100 L. Zhang, Z. J. Zhao and J. Gong, *Angew. Chem., Int. Ed.*, 2017, **56**, 11326–11353.
101 K. J. P. Schouten, Y. Kwon, C. J. M. van der Ham, Z. Qin and M. T. M. Koper, *Chem. Sci.*, 2011, **2**, 1902–1909.
102 Z. Fu, X. Wang, A. M. Gardner, X. Wang, S. Y. Chong, G. Neri, A. J. Cowan, L. Liu, X. Li, A. Vogel and R. Clowes, *Chem. Sci.*, 2020, **11**, 543–550.
103 K. Lei, D. Wang, L. Ye, M. Kou, Y. Deng, Z. Ma, L. Wang and Y. Kong, *ChemSusChem*, 2020, **13**, 1725–1729.
104 I. H. Chowdhury, A. H. Chowdhury, A. Das, A. Khan and S. M. Islam, *New J. Chem.*, 2020, **44**, 11720–11726.
105 Y. Xiang, W. Dong, P. Wang, S. Wang, X. Ding, F. Ichihara, Z. Wang, Y. Wada, S. Jin, Y. Weng and H. Chen, *Appl. Catal., B*, 2020, **274**, 119096.
106 L. J. Wang, R. L. Wang, X. Zhang, J. L. Mu, Z. Y. Zhou and Z. M. Su, *ChemSusChem*, 2020, **13**, 2973–2980.
107 M. Lu, Q. Li, J. Liu, F. M. Zhang, L. Zhang, J. L. Wang, Z. H. Kang and Y. Q. Lan, *Appl. Catal., B*, 2019, **254**, 624–633.
108 S. Q. You, J. Zhou, M. M. Chen, C. Y. Sun, X. J. Qi, A. Yousaf, X. L. Wang and Z. M. Su, *J. Catal.*, 2020, **392**, 49–55.
109 Z. Fu, X. Wang, A. M. Gardner, X. Wang, S. Y. Chong, G. Neri, A. J. Cowan, L. Liu, X. Li, A. Vogel, R. Clowes, M. Bilton, L. Chen, R. S. Sprick and A. I. Cooper, *Chem. Sci.*, 2020, **11**, 543–550.
110 Y. Huang, P. Du, W. X. Shi, Y. Wang, S. Yao, Z. M. Zhang, T. B. Lu and X. Lu, *Appl. Catal., B*, 2021, **288**, 120001.
111 N. Singh, D. Yadav, S. V. Mulay, J. Y. Kim, N. J. Park and J. O. Baeg, *ACS Appl. Mater. Interfaces*, 2021, **13**, 14122–14131.
112 K. Guo, X. Zhu, L. Peng, Y. Fu, R. Ma, X. Lu, F. Zhang, W. Zhu and M. Fan, *Chem. Eng.*, 2021, **405**, 127011.
113 L. Peng, S. Chang, Z. Liu, Y. Fu, R. Ma, X. Lu, F. Zhang, W. Zhu, L. Kong and M. Fan, *Catal. Sci. Technol.*, 2021, **11**, 1717–1724.
114 M. Fernández, A. Shamsabadi and V. Chudasama, *Chem. Commun.*, 2020, **56**, 1125–1128.
115 G. C. D. Bandomo, S. S. Mondal, F. Franco, A. Bucci, V. Martin-Diaconescu, M. A. Ortuño, P. H. van Langevelde, A. Shar, N. López and J. Lloret-Fillol, *ACS Catal.*, 2021, **11**, 7210–7222.
116 Y. Zhao, L. Hao, J. Ning, H. Zhu, A. Vijayakumar, C. Wang and G. G. Wallace, *Appl. Catal., B*, 2021, **291**, 119915.

117 M. Liu, Y. R. Wang, H. M. Ding, M. Lu, G. K. Gao, L. Z. Dong, Q. Li, Y. Chen, S. L. Li and Y. Q. Lan, *Sci. Bull.*, 2021, **66**, 1659–1668.
118 Q. Wu, M. J. Mao, Q. J. Wu, J. Liang, Y. B. Huang and R. Cao, *Small*, 2021, **17**, 2004933.
119 M. D. Zhang, D. H. Si, J. D. Yi, S. S. Zhao, Y. B. Huang and R. Cao, *Small*, 2020, **16**, 2005254.
120 Q. Wu, R. K. Xie, M. J. Mao, G. L. Chai, J. D. Yi, S. S. Zhao, Y. B. Huang and R. Cao, *ACS Energy Lett.*, 2020, **5**, 1005–1012.
121 H. J. Zhu, M. Lu, Y. R. Wang, S. J. Yao, M. Zhang, Y. H. Kan, J. Liu, Y. Chen, S. L. Li and Y. Q. Lan, *Nat. Commun.*, 2020, **11**, 1–10.
122 B. Han, X. Ding, B. Yu, H. Wu, W. Zhou, W. Liu, C. Wei, B. Chen, D. Qi, H. Wang and K. Wang, *J. Am. Chem. Soc.*, 2021, **143**, 7104–7113.
123 S. An, C. Lu, Q. Xu, C. Lian, C. Peng, J. Hu, X. Zhuang and H. Liu, *ACS Energy Lett.*, 2021, **6**, 3496–3502.
124 J. Huang and K. Pu, *Angew. Chem., Int. Ed.*, 2020, **132**, 11813–11827.
125 Y. Lu, J. Zhang, W. Wei, D. D. Ma, X. T. Wu and Q. L. Zhu, *ACS Appl. Mater. Interfaces*, 2020, **12**, 37986–37992.
126 M. Lu, M. Zhang, C. G. Liu, J. Liu, L. J. Shang, M. Wang, J. N. Chang, S. L. Li and Y. Q. Lan, *Angew. Chem., Int. Ed.*, 2021, **133**, 4914–4921.
127 B. Wang, F. Yang, Y. Dong, Y. Cao, J. Wang, B. Yang, Y. Wei, W. Wan, J. Chen and H. Jing, *Chem. Eng.*, 2020, **396**, 125255.
128 S. Q. You, J. Zhou, M. M. Chen, C. Y. Sun, X. J. Qi, A. Yousaf, X. L. Wang and Z. M. Su, *J. Catal.*, 2020, **392**, 49–55.
129 B. Han, X. Ding, B. Yu, H. Wu, W. Zhou, W. Liu, C. Wei, B. Chen, D. Qi, H. Wang and K. Wang, *J. Am. Chem. Soc.*, 2021, **143**, 7104–7113.
130 B. Han, Y. Jin, B. Chen, W. Zhou, B. Yu, C. Wei, H. Wang, K. Wang, Y. Chen, B. Chen and J. Jiang, *Angew. Chem.*, 2022, **134**, e202114244.
131 S. Y. Chi, Q. Chen, S. S. Zhao, D. H. Si, Q. J. Wu, Y. B. Huang and R. Cao, *J. Mater. Chem. A*, 2022, **10**, 4653–4659.
132 Q. Pan, M. Abdellah, Y. Cao, W. Lin, Y. Liu, J. Meng, Q. Zhou, Q. Zhao, X. Yan, Z. Liand and H. Cui, *Nat. Commun.*, 2022, **13**, 1–13.
133 H. Dong, M. Lu, Y. Wang, H. L. Tang, D. Wu, X. Sunand and F. M. Zhang, *Appl. Catal., B*, 2022, **303**, 120897.
134 (*a*) S. Kandambeth, D. B. Shinde, M. K. Panda, B. Lukose, T. Heine and R. Banerjee, *Angew. Chem., Int. Ed.*, 2013, **52**, 13052–13056; (*b*) H. Xu, J. Gao and D. Jiang, *Nat. Chem.*, 2015, **7**, 905.
135 (*a*) M. S. Lohse and T. Bein, *Adv. Funct. Mater.*, 2018, **28**, 1705553; (*b*) F. J. Uribe-Romo, C. J. Doonan, H. Furukawa, K. Oisaki and O. M. Yaghi, *J. Am. Chem. Soc.*, 2011, **133**, 11478–11481; (*c*) S. Kandambeth, A. Mallick, B. Lukose, M. V. Mane, T. Heine and R. Banerjee, *J. Am. Chem. Soc.*, 2012, **134**, 19524–19527; (*d*) Z. Li, Y. Zhang, H. Xia, Y. Mu and X. Liu, *Chem. Commun.*, 2016, **52**, 6613–6616.
136 J. Guo, Y. Xu, S. Jin, L. Chen, T. Kaji, Y. Honsho, M. A. Addicoat, J. Kim, A. Saeki, H. Ihee, S. Seki, S. Irle, M. Hiramoto, J. Gao and D. Jiang, *Nat. Commun.*, 2013, **4**, 2736.